# THE CAPTURE AND DECAY INTERACTIONS OF NEGATIVE MUONS STOPPED IN MATTER

by

N.H. Lipman, B.Sc.

A thesis presented for the degree of Ph.D. in the Faculty of Science of the University of Liverpool.

September, 1959.

# THE CAPTURE AND DECAY INTERACTIONS OF NEGATIVE MUONS STOPPED IN MATTER

by

N.H. Lipman, B.Sc.

A thesis presented for the degree of
Ph.D. in the Faculty of Science of
the University of Liverpool.

September, 1959.

## PREFACE

The experimental work described in this thesis was the result of collaboration between Mr. A. Astbury, Mr. M. Hussain, Mr. M.A.R. Kemp, Dr. H. Muirhead, Dr. R.G.P. Voss, Dr. C. Zangger and myself.

I am deeply grateful to my supervisor, Dr. H. Muirhead, for his constant guidance, advice and encouragement throughout my time of research.

## ABSTRACT

The present thesis is divided into two chapters, which deal with two aspects of the behaviour of negative muons brought to rest in matter.

In Chapter I the muon capture process ($\mu^- + p \rightarrow n + \nu$) is discussed, and an experiment is described in which muon capture rates were measured to accuracies of a few per cent for various target nuclei. The main interest of the experiment was to make a comparison between measured capture rates and the theoretically predicted capture rates of Tolhoek and Luyten. The theory is sensitive to the type of coupling that prevails in the muon capture process, and Tolhoek and Luyten have derived two values for the capture rate in each element considered, one for a Fermi type of coupling (pseudoscalar, scalar and vector) and the other for Gamow-Teller coupling (axial vector and tensor). A comparison between experiment and theory over a range of selected elements should in principle detect whether the coupling is pure Fermi, pure Gamow-Teller, or a mixture of the two. The results, in fact, favour an excess of the Gamow-Teller over the Fermi type of coupling.

In Chapter II the subject considered is the perturbation of the muon decay process ($\mu^- \rightarrow e^- + \nu + \bar{\nu}$) brought about by atomic binding. A muon in orbit within a muonic atom may be expected to decay at a modified rate; we have investigated this experimentally for negative muons stopped in aluminium, and in copper, and have shown that there is no deviation from the free muon decay rate within the experimental standard deviation of 5%.

TABLE OF CONTENTS

## LIST OF FIGURES

## LIST OF TABLES

## GENERAL INTRODUCTION

Two experiments are considered in the present thesis, which has in consequence been split into two separate chapters. Certain of the electronic and technical details are common to both experiments, and these have been given in detail only in Chapter I.

In Chapter I the muon capture process ($\mu^- + p \rightarrow n + \nu$) is considered, this being one of the three basic (strangeness conserving) 4-fermion interactions. The other two 4-fermion interactions, beta decay and muon decay, are already quite well understood; it is known that they both proceed through the same type of coupling (V-A), and that they have practically equal coupling constants. This similarity led to the Puppi theory of 'Universality' of the 4-fermion interactions,[1] and to the more recent theory of Gell-Mann of the 'conserved vector current' in the weak interactions[2]. Little is known experimentally about muon capture, and it has not yet been proved whether or not it fits correctly into the predicted scheme of 'Universality'. It has been our aim in the present experiment to measure absolute muon capture rates to a high accuracy, and thence by comparison with the theoretically predicted capture rates of Tolhoek and Luyten[3] to determine the coupling strength and coupling type of the muon capture interaction.

In the opening section of Chapter I, certain aspects of the currently held weak interaction theory have been briefly outlined, in order to show the type of behaviour which may be expected of muon capture.

In Chapter II the muon decay process is considered

$$\mu^- \rightarrow e^- + \nu + \bar{\nu}$$

for the special case in which the negative muon decays whilst in atomic orbit within a muonic atom. It is of interest to discover

whether the Coulomb field of the binding nucleus will disturb the decay process, thereby altering the transition rate of the interaction. There has been no complete theoretical solution to this problem. It was decided to measure 'bound muon' decay rates experimentally, as these were required in the analysis of the muon capture experiment of Chapter I.

* * *

# CHAPTER I

## CAPTURE RATES FOR NEGATIVE MUONS IN VARIOUS ELEMENTS

## SECTION 1 : INTRODUCTION

### 1 a) Weak Interaction Theory - General

Following the discovery of parity violation, a considerable amount of progress has been made in the theoretical and experimental understanding of the weak interactions.

One of the most significant facts that has emerged is that the coupling constants for all measured weak interactions are practically equal. Further, it appears that the type of coupling (V-A) is the same for all the cases which have been completely analysed[2,4]. These discoveries have led to the hypothesis of the 'Universality' of the weak interaction, by which is meant that the various weak interactions are all essentially one and the same, with only the names of the participating particles changed. This theory only stands so long as each weak interaction can be shown to have the same coupling constant and coupling type as all the others (apart from renormalization effects).

The basic weak interaction is considered to be an interaction between 4 fermions. An example is muon decay ($\mu \to e + \nu + \bar{\nu}$) which is represented by a Feynman diagram of the following type:

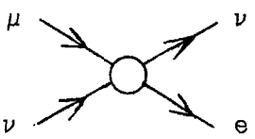


Other weak decay modes are believed to involve at some stage a 4-Fermion interaction. For example, the decay of the $\pi$ meson has the following Feynman graphs

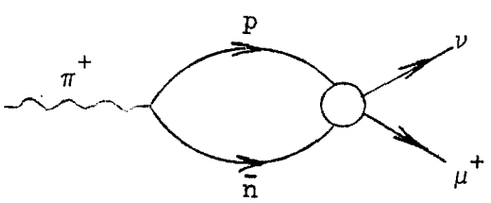


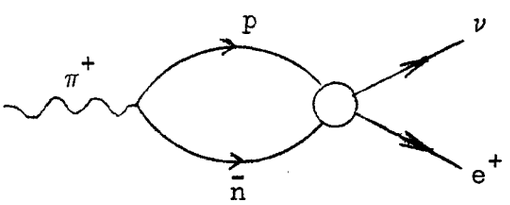

The pion is considered to have a strong interaction in which a virtual nucleon-antinucleon pair is produced, and then these interact by a 4-fermion process to produce a lepton-antilepton pair.

There are three basic (strangeness conserving) 4-fermion interactions, $\mu\nu e\nu$, $npe\nu$, and $np\mu\nu$, of which only the first two have been analysed experimentally. It is essential to the acceptance of 'Universality' that the third interaction, muon capture, should be shown to have the same coupling constant and coupling type as the other two. This has been the aim of the present experiment.

Some of the properties of the 4-fermion interaction have been briefly outlined in the sub-section that follows. Muon capture is considered again explicitly in sub-sections 1 g) and 1 h).

1 b) 4-Fermion Interaction Theory

The basic weak interactions are characterized by interaction Hamiltonian densities of the form[5]

$$H_I(r) = g \sum_{i,j,k,l} C_{ijkl}\, \Psi_a^{*(i)}(\underline{r})\, \Psi_b^{(j)}(\underline{r})\, \Psi_c^{*(k)}(\underline{r})\, \psi_d^{(\ell)}(\underline{r}) \qquad (1)$$

where the subscripts a,b,c,d refer to the 4 fermions involved in the interaction, $\Psi_b^{(j)}(\underline{r})$ is the j th. component of the spinor field operator which destroys a particle in state b, etc., and g is the coupling constant having a magnitude of the order of $10^{-49}$ erg cm$^3$. The $C_{ijkl}$ are constants and are in general complex.

The total Hamiltonian is given by:

$$\mathcal{H}_I = \int H_I \cdot d\tau \,. \qquad (2)$$

If we require that the Hamiltonian be invariant under proper Lorentz transformations, then only certain combinations of the products in Eq. 1 will be allowed. In practice, all the possible forms of $H_I$, which are invariant under proper Lorentz transformations, can be described by the equation

$$H_I = g \sum_{i=1 \text{ to } 5} \Big[ C_i \Big( \psi_a^*(\underline{r})\, O_i\, \psi_b(\underline{r}) \Big) \Big( \psi_c^*(\underline{r})\, O_i\, \psi_d(\underline{r}) \Big) + C_i' \Big( \psi_a^*(\underline{r})\, O_i\, \psi_b(\underline{r}) \Big) \Big( \psi_c^*(\underline{r})\, O_i\, \gamma_5\, \psi_d(\underline{r}) \Big) + \text{h.c.} \Big] \quad (3)$$

where $O_i$ are Dirac operators, and have the following transformation properties:

| | |
|---|---|
| Scalar | $O_1 = \gamma_4$ |
| Vector | $O_2 = \gamma_4\gamma_\mu$ |
| Tensor | $O_3 = \gamma_4(\gamma_\mu\gamma_\nu - \gamma_\nu\gamma_\mu) \quad \mu \neq \nu$ |
| Axial vector | $O_4 = \gamma_4\gamma_5\gamma_\mu$ |
| Pseudoscalar | $O_5 = \gamma_4\gamma_5$ . |

The $\gamma_\mu$ are anti-commuting operators defined by the Dirac equation [6].

The constants $C_i$ and $C_i'$ will in general be complex, but if the Hamiltonian is invariant under time reversal they will be real.

If the Hamiltonian were further required to be invariant under the parity transformation (i.e. reflection), then the coefficients $C_i'$ would be identically zero.

By integrating the time dependent Schrödinger equation, and bearing in mind that the interaction is weak, we find that the probability per unit time of finding an assembly of particles in

state $\Psi_f$ when it was initially in state $\Psi_i$ is given by:

$$dn/dt = \frac{2\pi}{\hbar} |M_{fi}|^2 \, dn/dE$$

where $dn/dE$ is the energy density of the final states, and $M_{fi}$ is the matrix element for the transition and is given by:

$$M_{fi} = \langle \Psi_f | \mathcal{H}_I | \Psi_i \rangle . \qquad (4)$$

$\Psi(f)$ and $\Psi(i)$ are the wave functionals of the initial and final states respectively.

In treating a physical problem in which the initial and final states are specified explicitly, only those terms in the Hamiltonian which transform the initial wave functional into the final wave functional (or some multiple of it) will produce non-zero matrix elements. Each of the particle operators consists of the product of a creation and destruction operator with a Dirac spinor wave function. For any specified transition the action of the creation and destruction operators is taken into account in deciding which matrix elements will be non-vanishing; the remaining part of the calculation of the matrix element will involve the use of the Dirac wave functions only. Thus in any case in which the problem is explicitly specified the matrix element will be of the form:

$$M_{fi} = g \int \sum_i \Big[ C_i \Big( \bar{U}_a(\underline{r}) \, O_i \, U_b(\underline{r}) \Big) \Big( \bar{U}_c(\underline{r}) \, O_i \, U_d(\underline{r}) \Big) + C_i' \Big( \bar{U}_a(\underline{r}) \, O_i \, U_b(\underline{r}) \Big) \Big( \bar{U}_c(\underline{r}) \, O_i \, \gamma_5 \, U_d(r) \Big) \Big] \, d\tau \qquad (5)$$

where $U_b$ and $U_d$ are the wave functions of the particles which were destroyed, and $\bar{U}_a$ and $\bar{U}_c$ are the hermitian conjugate wave functions of the particles which were created.

It will be noticed in the above equation that the complex conjugate terms do not occur, due to the fact that their associated operators produce the inverse reaction and thus cannot connect the specified initial and final states.

1 c) Universality

It has been pointed out that the coupling constants for the various weak interactions are equal, within the accuracy of the experimental measurements. This has led to the suggestion that the weak interactions are not just similar to each other, but are essentially identical, and must therefore all be described by the same interaction Hamiltonian, with the same coupling type and coupling constant applying in each case[1,2,7,8].

For a given interaction the deductions that can be made from the experimental data with regard to the coupling type are not unique, but depend on the order given to the spinor operators in the interaction Hamiltonian. For each change of ordering one obtains a new set of coupling coefficients ($C_S$, $C_V$, $C_T$, $C_A$, $C_P$), a linear combination of the old, which will allow agreement between experiment and theory[9,10]. It may be shown that in the special case of a V-A theory ($C_S = C_P = C_T = 0$; $C_V = - C_A$) all orderings of the Hamiltonian are equivalent[10,2]. Thus a 'Universal' V-A theory is the simplest theory possible, as it does not depend on the orderings which one chooses for the Hamiltonians of the various weak interactions.

1 d) Non-Conservation of Parity in Weak Interactions

It will be seen in Eq. 5 that if parity is not conserved in weak interactions the matrix element will contain two types of term :

i) the "even" terms have coefficients $C_i$, and behave as scalars;

ii) the "odd" terms have coefficients $C_i'$, and behave as pseudo-scalars.

The evaluation of any physical quantity will involve the use of a matrix element squared. The calculation of a quantity of pseudo-scalar kind (e.g. $\underline{\sigma} \cdot \underline{p}$) must involve cross products between the "odd" terms and the "even" terms, because only such products can behave as pseudo-scalars. Thus the experimental measurement of a non-zero pseudoscalar quantity will be a direct proof that the "odd" and "even" terms co-exist in the interaction Hamiltonian, and hence that parity is not conserved by the interaction[11].

It is apparent by a direct physical argument that if a quantity of the type $\underline{\sigma} \cdot \underline{p}$ exists, then it will appear to have the opposite sign when reflected in the origin and will thus be non-invariant under the parity operation.

The measurement by Wu et al.[12] of the electron emission asymmetry for the beta decay of polarized $Co^{60}$, and the measurement by Garwin et al.[13] of the electron emission asymmetry for the decay of stopped muons, have proved that parity is not conserved in beta decay, muon decay, and pion decay.

Rapid progress has recently been made in the measurement of the various quantities involved in beta decay and muon decay, and an analysis of the resulting data has led to the development of a concise phenomenological theory of the weak interactions. The most recent summary of the position has been given by Goldhaber (1958 CERN Conference)[4]. In the present thesis I only intend to quote some of the more important results.

It is found from measurements of pseudoscalars that maximal violation of parity exists in the weak interactions: this would be given by the coefficients of the "odd" and "even" terms in the interaction Hamiltonian being equal in magnitude. The interaction Hamiltonian will thus reduce to the form:

$$H_I = \sum_i C_i \left(\bar{\Psi}_a \, O_i \, \Psi_b\right)\left(\bar{\Psi}_c \, O_i \, (1 \pm \gamma_5) \, \Psi_d\right) . \qquad (6)$$

The factor $(1 \pm \gamma_5)$ is the projection operator for a right/left-handed neutrino; and with the problem in this form the simplest analysis of the experimental data may be obtained on the basis of the two-neutrino theory with lepton conservation. We find that the $e^-$, $\mu^-$ and left-handed neutrino ($\nu$ or $\nu_L$) all belong to the same group, which we designate as the leptons, and the $e^+$, $\mu^+$, and right-handed neutrino ($\bar{\nu}$ or $\nu_R$) belong to the antilepton group. It is required that in an interaction the number of leptons minus the number of antileptons must remain a constant. Thus in an interaction involving a single neutrino only one type of neutrino (i.e. $\nu$ or $\bar{\nu}$) can take part. A comparison between experiment and theory for beta decay and muon decay shows that in each case the coupling is a mixture of vector and axial vector types.

1 e) Beta Decay

The $\beta^+$ decay process is described by the equation:

$$p \rightarrow N + e^+ + \nu .$$

The interaction Hamiltonian is normally written:

$$H_I = \sum_i C_i \left(\Psi^*_N \, O_i \, \Psi_p\right)\left(\Psi^*_\nu \, O_i \, \Psi_{e^-}^{(-ve)}\right) \qquad (7)$$

where $\Psi_\nu^*$ is the creation operator for a left-handed neutrino in the state $U_\nu$, and $\Psi_{e^-}^{(-ve)}$ is an operator which destroys an $e^-$ in a negative energy state (this is equivalent to creating an $e^+$ in a positive energy state).

Some of the results which were used in the logical development of the theory are listed below.

i) Goldhaber's measurements on K capture in $Eu^{152}$ established that the particle $\nu$ is left-handed[14].

ii) The measurements of electron emission asymmetries and of electron polarization[15], in conjunction with result i) established that the coupling in $\beta$ decay is a mixture of vector and axial vector types.

iii) The results of electron-neutrino correlation experiments were originally contradictory, but the $He^6$ experiment has recently been repeated[16] and the old measurement has been withdrawn; all the results are now in agreement, and favour a V,A mixture[17].

iv) The measurements of the Ft values for the $\beta$ decay of $O^{14}$, $Al^{26}$, and $Cl^{34}$, all of which are super-allowed transitions with almost pure Fermi coupling, yield a value for the vector coupling constant[18]

$$C_V = 1.410 \pm .009 \times 10^{-49} \text{ erg cm}^3.$$

v) The most recent measurement of the half-life of the neutron ($t = 11.7 \pm .3$ min)[19] gives an Ft value for the $\beta$ decay of the neutron of 1170; this result in conjunction with result iv) gives the ratio of the Fermi and Gamow-Teller coupling constants

$$(C_{G.T.})^2 / (C_F)^2 = 1.55 \pm .08 .$$

vi) The measured $e^- - \bar{\nu}$ correlation for the decay of polarized neutrons indicates that the coefficients $C_A$ and $C_V$ have opposite signs within a phase angle of $\pm 8^\circ$ [20].

vii) The measured emission asymmetry of the electrons from the decay of polarized neutrons (together with the measured $\bar{\nu}$ asymmetry) yields the relation [4,21]:

$$C_V = -1.25 \pm .04\, C_A .$$

From the above results it is seen that the nature of the beta decay process is now well known in terms of the interaction Hamiltonian. What the physical significance of the Hamiltonian in its present form may be has yet to be established.

1 f) Muon Decay

The muon decay process is described by the equation:

$$\mu \rightarrow e + \nu + \bar{\nu} .$$

The measurement of the $\rho$ parameter confirms that a $\nu$ and a $\bar{\nu}$, rather than two $\nu$'s or two $\bar{\nu}$'s are emitted in the decay [4,22,23].

The interaction Hamiltonian density is normally given the following ordering:

$$H_I = \sum_i C_i \left(\Psi_\nu^* \, O_i \, \Psi_\mu\right)\left(\Psi_e^* \, O_i \, \Psi_\nu^{(-ve)}\right) . \qquad (8)$$

The measurements of the electron spirality [4,24] and the electron emission asymmetry [25] for $\mu^+$ decay and $\mu^-$ decay, yield the same spiralities for the $\bar{\nu}$ and the $\nu$ as those given by $\beta$ decay results. The value and sign of the $\xi$ parameter is such as to require a mixture

of vector and axial vector couplings, with the V and A coefficients approximately equal and opposite in sign (i.e. $C_V \doteqdot -C_A$)[26].

It is seen that the two interactions, $\beta$ decay and $\mu$ decay, appear to behave alike, thus lending strength to the hypothesis of 'Universality' which now predicts that 'V-A' coupling will prevail in all the weak interactions.

1 g) Muon Capture

The muon capture process is described by the equation

$$\mu^- + p \rightarrow N + \nu$$

where the proton and the neutron may be bound or free. The presence of a zero mass particle is demanded by the fact that the measured excitation energy of the final system appears to be much less than the rest energy of the muon, and thus most of the energy must have been taken away by a neutrino. It will be seen that the capture process, as written above, conserves leptons.

The interaction Hamiltonian density is given the following ordering:

$$H_I = \sum_{i=1 \text{ to } 5} C_i \, (\Psi_n^* \, O_i \, \Psi_p)(\Psi_\nu^* \, O_i \, \Psi_\mu) \qquad (9)$$

where the operators $\Psi_n^*$ and $\Psi_p$ may refer to bound or unbound nucleons, as the case may be.

Little experimental information has been obtained on the muon capture process; it is not known whether the 'V-A' interaction mixture applies, nor has it been proven that parity is violated in the interaction.

If parity is not conserved then for polarized muons captured, the emitted neutrons will have an asymmetric spacial distribution. In particular, in the case of muons captured in hydrogen, the angular distribution is given by:

$$\frac{d\sigma(\Theta)}{d\Omega} \propto (1 + P\alpha \cos\Theta) \qquad (10)$$

where $\Theta$ is the angle between the direction of the muon beam and the direction of emission of the neutron, P is the polarization of the muons on reaching the ground state of the mesonic atoms, and $\alpha$ is the asymmetry parameter which in the case of a 2-neutrino theory is given by [27]:

$$\alpha = \left(|C_S + C_V|^2 - |C_T + C_A|^2\right) \Big/ \left(|C_S + C_V|^2 + 3|C_T + C_A|^2\right) . \qquad (11)$$

For pure Fermi coupling $\alpha$ is 1, for pure Gamow-Teller coupling $\alpha$ is $-\frac{1}{3}$, and for equal parts of Fermi and Gamow-Teller couplings $\alpha$ is zero. It is perhaps unfortunate that if the asymmetry parameter can be measured then the value obtained will be close to zero, if the $\beta$ interaction ($C_A = -1.2\, C_V$) applies; an asymmetry of zero could imply that the interaction conserves parity.

In practice the measurement of the neutron asymmetry for muons stopped in hydrogen will be extremely difficult if not impossible, for it has been shown that muons stopped in liquid hydrogen become completely depolarized [28], and further, the fraction which will undergo capture rather than decay will be vanishingly small ($F_{captured} \doteqdot 0.01\%$).

It should be possible to measure neutron asymmetries for muons captured in elements such as silicon, for which the capture rate is approximately equal to the decay rate, so that some 50% of the incoming negative muons will be captured; it is known that muons

stopped in silicon have a residual polarization of approximately 20%[29]. An experiment of this type is being done at present by the group headed by H. Muirhead; the analysis will be less certain than that for the case of hydrogen, as the nuclear properties of the initial proton and the final neutron must be taken into account.

1 h) Capture Rates

Tolhoek and Luyten[3] have calculated capture rates for negative muons in a range of elements from calcium to nickel using shell model wave functions for the initial and final nuclear states involved. They found that the capture rates were sensitive to the coupling type, and pointed out that by a suitable comparison between experimental measurements and their theoretical predictions it would be possible to determine the ratio of Fermi to Gamow-Teller couplings ($C_F^2/C_{G.T.}^2$) for the muon capture interaction.

The capture rate is given by:

$$\lambda_c = \int_{fi} \frac{2\pi}{\hbar} |M_{fi}|^2 \rho_f \qquad (12)$$

where $M_{fi}$ is the matrix element for a transition between a definite initial proton state and a definite final neutron state, and $\int_{fi}$ denotes a summation over all the transitions that contribute for a given target element. The matrix elements squared for the individual transitions are given in Table 1 of Tolhoek and Luyten's paper, and the calculated capture rates for pure Fermi and pure Gamow-Teller couplings, for the cases of pure targets, and targets of naturally occurring isotopic mixtures are given in Tables 2 and 4. Table 4 is reproduced below and is designated Table I for the purpose of the present thesis.

It will be seen that in the case of calcium the Gamow-Teller coupling gives exactly three times the capture rate predicted by Fermi

TABLE I

Predicted muon capture rates for Fermi coupling, $\lambda_c(S,V)$, and Gamow-Teller coupling, $\lambda_c(T,A)$.

| Element | $\lambda_c(T,A)/3 \times 10^{101}$ $g^2$ | $\lambda_c(S,V)/10^{101}$ $g^2$ |
|---|---|---|
| Ca | 145 | 145 |
| Sc | 136 | 130 |
| Ti | 147 | 128 |
| V | 150 | 111 |
| Cr | 185 | 130 |
| Mn | 207 | 137 |
| Fe | 246 | 157 |
| Co | 268 | 165 |
| Ni | 320 | 194 |

coupling. It is convenient to express the capture rates for the various elements as ratios to the calcium rates (see Table V). If the coupling actually responsible for muon capture is a mixture of Fermi and Gamow-Teller interactions, then the capture rate will be given by:

$$\lambda_c = |C_S + C_V|^2 \lambda_c(S,V) + |C_A + C_T|^2 \lambda_c(T,A) \qquad (13)$$

where $\lambda_c(S,V)$ and $\lambda_c(T,A)$ are the capture rates due to pure Fermi and Gamow-Teller interactions respectively.

A simpler theory has been derived by Primakoff based on a Fermi gas model of the nucleus which predicts muon capture rates in elements throughout the periodic table. (Reported by Sens et al., 1957[30].) This theory is insensitive to the type of coupling that prevails in the interaction, and gives capture rates in accordance with the formula:

$$\lambda_c(A,Z) = \lambda_c(1,1)\, \gamma Z_{eff}^4 \left(1 - \delta \frac{A-Z}{2A}\right) \qquad (14)$$

where $\lambda_c(1,1) = 220$ is obtained from $\beta$ decay results, and $\gamma$ and $\delta$ are calculated constants having the values of 0.73 and 3 respectively[32]. The Primakoff theory is expected to hold in an average way rather than for each individual nucleus, as it does not take into account discontinuities brought about by the shell structure of the nucleus.

Sens, Swanson, Telegdi and Yovanovitch[30] have measured muon capture rates for a large range of elements, and their results are on the whole in good agreement with the predictions of Primakoff. The results of the present experiment,[31] and of Telegdi's experiment,[30] are in good agreement with the capture rates predicted by Tolhoek and Luyten for the case of Gamow-Teller coupling.

* * *

## SECTION 2 : EXPERIMENTAL METHOD

### 2 a) Principle of the Measurement

When a negative $\mu$ meson comes to rest in a target it is captured into orbit around a target nucleus, thus forming a mesic atom. It then cascades down to the Bohr orbit of the atom in a time of the order of $10^{-10}$ seconds. In this condition the muon will suffer one of two fates:

i) it may decay with the emission of an electron, a neutrino, and an antineutrino, for which the probability is $\lambda_d$; or

ii) it may interact with the nucleus converting a proton into a neutron with the emission of a neutrino, for which the probability is $\lambda_c$.

As a result of the two processes, negative muons which come to rest in a target will be lost at a net rate $\lambda_L$, given by:

$$\lambda_L = \lambda_c + \lambda_d \quad . \qquad (15)$$

Consider a burst of muons $N_o$ arriving in a target at some instant in time, then the number $N_t$ remaining at time t later is given by:

$$N_t = N_o \, e^{-\lambda_L \cdot t} \quad . \qquad (16)$$

The number of muons decaying at any instant will be proportional to the number present, and will thus follow the above equation. The muon loss rate $\lambda_L$ was therefore determined by measuring the time distribution of the decay electrons from muons stopped in a target.

The value of the muon decay rate $\lambda_d$ is known from measurements on the decay of free muons ($\lambda_d = 4.5 \times 10^5/\text{sec}$)[33]. However, in

the present case the muon decay process will be perturbed by the Coulomb field of the binding nucleus. The measurement of the 'bound muon' decay rate is discussed in Chapter II. The required interaction rate $\lambda_c$ may be obtained from the measured values of $\lambda_L$ and $\lambda_d$. It should be noted that for most of the targets considered $\lambda_c >> \lambda_d$, and thus the value of $\lambda_c$ obtained is relatively insensitive to the value of $\lambda_d$ used.

2 b) The Cyclotron Beam

The external negative meson beam of the Liverpool Synchro-cyclotron was used for the experiment. This beam consists of approximately 86% $\pi$ mesons, 11% electrons and 3% $\mu$ mesons, and is produced by allowing the internally circulating proton beam to fall upon a beryllium target placed inside the cyclotron tank. Negatively charged particles which are emitted in the forward direction are bent away from the cyclotron by the fringing magnetic field. Those within a limited momentum range pass through a duct in the screening wall, into the experimental room. The pions, muons and electrons in the beam thus have similar momenta.

The beam is not continuous in time but comes in bursts of approximately 250 $\mu$sec duration, which are repeated 100 times a second. As a result the beam has a mark space ratio of approximately 40, which must be taken into account in the calculation of random coincidence rates, and dead-time losses in the experimental apparatus.

Each mark pulse has a fine structure; during a mark pulse particles arrive in bursts of the order of 12 m $\mu$sec duration, with a repetition frequency of $20 \times 10^6$/sec. The fine structure of the beam must also be taken into account in the calculation of random coincidence rates, etc.

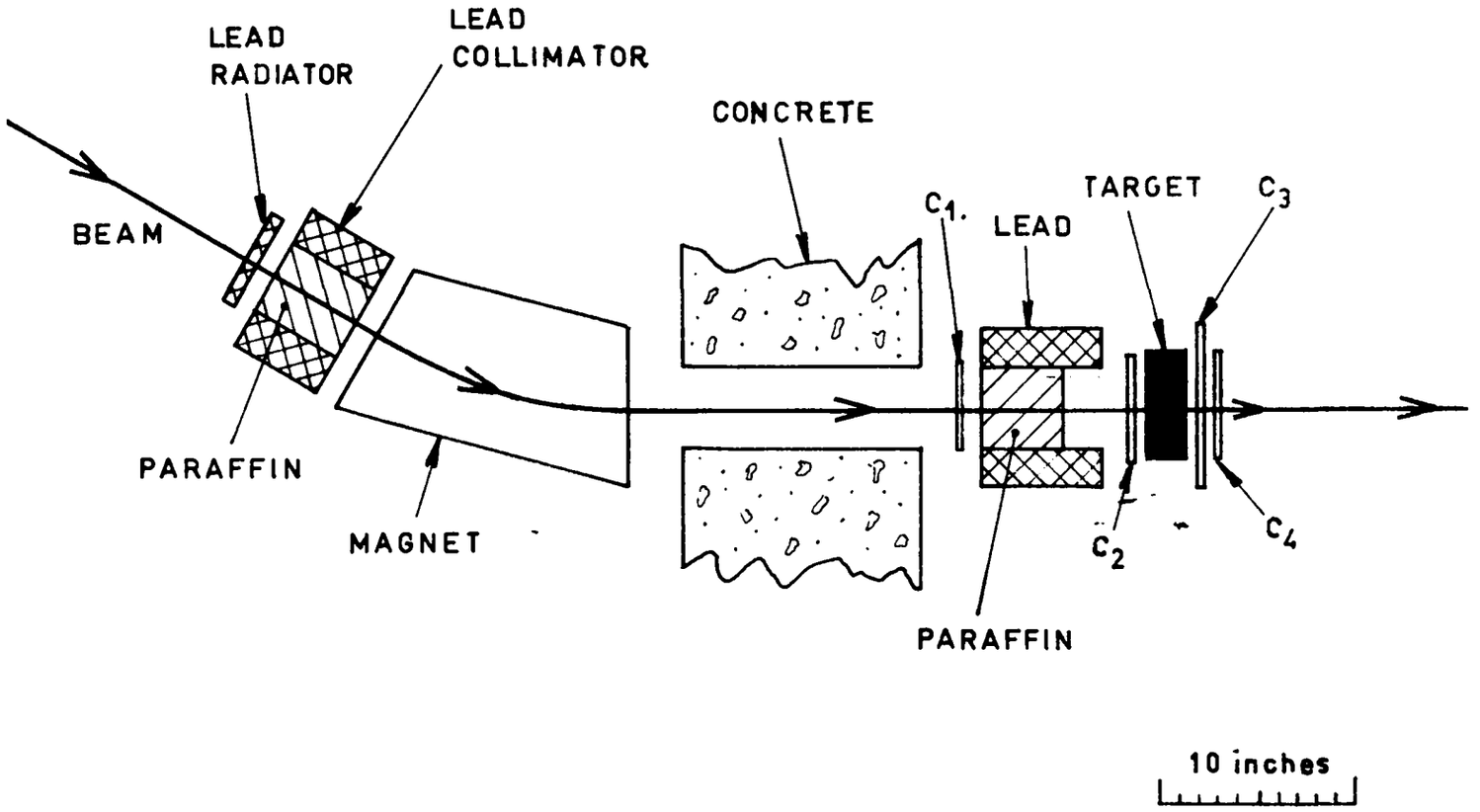


Fig.1 Experimental layout.

2 c) The Apparatus - General

The experimental arrangement is shown in Fig. 1. The beam passed through a $\frac{1}{2}$-inch thick lead sheet before entering the bending magnet. The lead caused most of the electrons in the beam to radiate energy, and thereby lose momentum; it was then possible by means of the bending magnet to momentum-separate the wanted muon beam from the unwanted electron contamination. The total absorber thickness was adjusted in conjunction with the bending magnet current to give the maximum number of $\mu$ mesons stopping in the target. The absorber thickness was sufficient to prevent most of the $\pi$ mesons present in the beam from reaching the apparatus.

The arrival of a muon in the target was signalled by a coincidence between counters 1 and 2, with counter 3 in anticoincidence. The emission of a delayed decay electron was signalled by a coincidence between counters 3 and 4 with counter 2 in anticoincidence. The signals from the muon and electron telescopes were fed into an electronic device (to be referred to hereafter as a timesorter) which gave a pulse out having a height proportional to the time delay between the two input pulses. The output from the timesorter was displayed on a 72-channel kicksorter.

The pattern obtained on the kicksorter represented a curve of the form

$$N_t = N_o \, e^{-\lambda_L \cdot t} + \text{background} \qquad (17)$$

where $N_t$ is the number of counts in the $t_{th}$ kicksorter channel, $N_o$ is the number in the channel corresponding to instantaneous time, and $\lambda_L$ is the required muon loss rate in terms of the time width of a kicksorter channel. The timesorter was calibrated by use of a double pulse generator, and hence the value of $\lambda_L$ was derived.

2 d) Counting Rate Problems

The greatest difficulty in the experiment was in obtaining a sufficiently high events rate in association with a fairly low random coincidence rate. The problem arose from the fact that after the occurrence of a muon count the apparatus had to remain sensitive for several $\mu$sec in order to detect the possible decay electron, and during this time a random count was liable to occur due to a spurious particle passing through the electron telescope.

It is of interest to discuss the actual counting rates obtained with the final experimental arrangement, in order to understand why this arrangement was decided upon. Muon decays were detected at a rate of two or three a second. Of the muons stopping in a target, a fraction $\frac{\lambda_d}{\lambda_c + \lambda_d}$ decay; thus for most of the elements considered approximately one-tenth of the incoming muons decayed. Taking into account the solid angle subtended at the target by the electron telescope, only one-fiftieth of the incoming muons will have produced detectable decays, and thus the muon flux must have been between 100 and 150 particles a second. The muon telescope actually counter at three times this rate, the extra particles being residual pions and electrons. There was a counting rate in the electron telescope of 40 particles a second, due to the general background in the experimental room, which was produced in part by the extracted pion beam, and in part by the circulating beam of the cyclotron.

The random counting rate is given by:

$$R = N_1 \cdot N_2 \cdot T \cdot S \qquad (18)$$

where $N_1$ and $N_2$ are the counting rates for the muon and electron telescopes, S is the mark space ratio for the meson beam, and T is the length of the timesorter time base. Taking the figures of

$N_1$ = 400/sec, $N_2$ = 40/sec, S = 40, and T = 2 $\mu$sec, the random coincidence rate is equal to 1.28 counts/sec which is approximately half the real events rate. The 2 $\mu$sec range was used for the measurements in nickel, cobalt and copper, the mean lives being of the order of 150 m$\mu$sec. It should be noted therefore that 95% of the decay events occurred over a time range of only 450 m$\mu$sec, and over this range the reals to randoms ratio was approximately 8 : 1.

2 e) Absorbers and Collimators

The muons entering the experimental room had a range of energies around 110 MeV; it was necessary to pass them through a considerable thickness of absorber in order to bring them to rest in the target. Paraffin was chosen as the absorber material because it gives a small amount of multiple scattering and has a relatively high stopping ability. Two absorber arrangements were tried; in the first the paraffin was placed directly in front of counter 1, and in the second there were 4" of paraffin between counters 1 and 2, and $7\frac{1}{2}$" on the cyclotron side of the bending magnet. The first arrangement had the advantage over the second in that fewer of the muons were lost by multiple scattering in the absorber, due to the fact that the absorber was closer to the muon telescope. However, the other beam particles were similarly favoured, and thus no net improvement was obtained. The second arrangement was found to be the better of the two due to the fact that most of the pions were lost well away from the apparatus, and thus the interactions which the stopped pions had with nuclei were less likely to produce spurious counts in the electron and muon telescopes.

A further improvement was obtained by including a $\frac{1}{2}$" thick lead radiator as part of the absorber in front of the bending magnet. This lead thickness corresponds to two radiation lengths for electrons, and thus approximately 90% of the electrons radiated. The resulting

loss of momentum prevented most of the electrons from reaching the muon telescope due to the momentum selection property of the bending magnet. By use of the lead radiator the random background rate was reduced by a factor two, for the same real events rate.

Three collimators were used with the apparatus: they are marked A, B and C on the diagram of the experimental arrangement shown in Fig. 1. Collimator A stopped those pions which scattered out of the sides of the first absorber; before the introduction of A it was found that a considerable number of pions were reaching the target by this means. Collimator B had the purpose of stopping particles which had the wrong momenta or which were scattered out of the beam. It thus prevented these particles from causing spurious counts in the apparatus. Collimator C was used to define the size of the beam entering the target. It had a smaller diameter than counter 2, and thus ensured that any beam particles reaching the electron telescope would be seen and "vetoed" by counter 2.

2 f) Scintillation Counters

Polystyrene scintillators ¼" thick and circular in section were used in the four counters; the diameters were $4\frac{1}{2}$", 5", $8\frac{1}{2}$" and $5\frac{1}{2}$" respectively. The light pulses from the scintillators were fed to the photocathodes of E.M.I. type 6260 photomultipliers through perspex light guides. The photomultipliers were screened from stray magnetic fields by concentric mu-metal and soft iron shields. The scintillators were covered by close-fitting "hats" made of .010" brass. The counters were mounted with the photomultiplier axes horizontal, which enabled pairs of scintillators to be brought very close together, as was required in the case of counters 3 and 4.

Pulses with a height of approximately half a volt, and a rise time of 10 mμsec were obtained from the last dynodes of the photomultipliers. The pulses were passed through head amplifiers,

and linc amplifiers to reach the coincidence circuit with a height of approximately 4 volts. Two coincidence circuits were used, one for the muon telescope, and the other for the electron telescope. The outputs from the two circuits will be referred to hereafter as "start" pulses and "stop" pulses, or as $12\bar{3}$ events and $\bar{2}34$ events, respectively.

Counter 3 was included as a "veto" counter in the muon telescope in order to prevent beam particles which passed right through the target from producing spurious "start" pulses. A large scintillator was used in 3 to enable the "vetoing" of beam particles which were scattered out of the sides of the target.

Two counters in coincidence were used to detect the decay electrons for the following reasons:

i) with two counters the background due to low-energy particles and photomultiplier noise is reduced, and the solid angle over which background particles are seen is also reduced;

ii) greater reliability of height and rise time is assured for the stop pulses;

iii) the detection efficiency for neutrons and $\gamma$-rays produced by the muon capture interaction is greatly reduced. This is an important consideration for the experiment discussed in the next chapter.

## 2 g) Targets

Muon mean lives were measured in fluorine, aluminium, calcium, vanadium, manganese, cobalt, nickel and copper. The targets used differed quite widely in their physical characteristics according to the materials available. The calcium target was obtained as a solid metal block, and the aluminium and copper targets were each made

up of several sheets of material. The nickel was in pellet form, the manganese and cobalt were in small jagged pieces, and the vandium was obtained as a powder. Lead fluoride, in powder form, was used for the measurement in fluorine. The presence of the lead did not disturb the measurement, because the muon mean lives in lead and fluorine are very different and therefore separable. The non-solid target materials were contained in perspex boxes, which had walls 0.3 gm/cm$^2$ thick.

The momentum spectrum of the muon beam was found to be such that most of the muons could be stopped within a target having a thickness of the order of 12 gm/cm$^2$. The targets were designed with this in mind; they are listed with their physical characteristics in Table II. The targets were square in section in the plane perpendicular to the beam. Certain targets had to be thicker than others to give the required stopping power; the extra thickness was a disadvantage, as it meant that the solid angle subtended by the electron telescope at the centre of the target was reduced.

TABLE II

Target Characteristics

| Material | Front Section | Thickness inches | Thickness gm/cm$^2$ | Purity |
|---|---|---|---|---|
| Lead fluoride | 4.6" × 4.6" | 2.5" | 14.2 | 99% |
| Aluminium | 9" × 9" | 1.4" | 9.0 | 99% |
| Calcium | 5" × 5" | 4" | 15.8 | 99% |
| Vanadium | 4.6" × 4.6" | 2.5" | 13.5" | 99.5% |
| Manganese | 4.6" × 4.6" | 1.3" | 10.1 | 99.9% |
| Cobalt | 4.6" × 4.6" | 1.3" | 14.6 | 99.6% |
| Nickel | 4.6" × 4.6" | 1.3" | 14.5 | 99.9% |
| Copper | 5" × 5" | 4.0" | 17.2 | 99% |

2 h) Carbon Background

The pattern obtained on the kicksorter represented a curve:

$$N_t = N_0 e^{-\lambda_L \cdot t} + N_0^* e^{-\lambda_L^* \cdot t} + C \qquad (19)$$

where $\lambda_L$ is the muon loss rate in the target material, $\lambda_L^*$ is the muon loss rate in carbon, and $N_0$, $N_0^*$, and C are constants. The constant term (C) was due to random coincidences between the muon and electron telescopes. The second term arose from muons coming to rest, and decaying in carbon. In the case of the target materials contained in perspex boxes the carbon background was expected to occur. However, a carbon background was also obtained with the solid calcium and copper targets. This may possibly have resulted from muons which came to rest just within the scintillator of counter 3 - the aforesaid muons losing too little energy in the scintillator to produce the required "veto" pulse in the muon telescope. These muons would disappear with the characteristic loss rate in carbon, and the resulting decay electrons would be detected over a large solid angle. It was suggested that the muons which found their way into counter 3 did so as a result of scattering out of the sides of the target, and thus if the target were made larger than counter 3 the carbon background would be removed. A measurement was therefore made with an aluminium target having a front section of 9" × 9" and no carbon background was detected.

2 i) Measurement of the Random Background

The random background C represented approximately one-third of the total counts obtained on the kicksorter. A technique was applied by which the random background could be measured concurrently with the lifetime, as follows.

A delay cable was inserted between the electron telescope and the timesorter, causing "stop" pulses to be delayed by several hundred mμsec. An event occurring simultaneously in the muon and electron telescopes would register as a count in the kicksorter channel representing the inserted time delay; to be referred hereafter as the "zero time" channel. In the case of a muon decay event the electron telescope would always give a count later than, or simultaneous to the count in the muon telescope, and thus muon decays would register in or beyond the zero time channel. On the other hand, random coincidences between the two telescopes would appear without favour in all the kicksorter channels. Thus the counts occurring in the channels preceding "zero time" gave a direct measurement of the random background C.

The length of the delay cable was chosen so as to position "zero time" at approximately one-sixth of the way along the timesorter time base, corresponding to some twelve channels along on the 72-channel kicksorter.

2 j) Positioning "Zero Time"

In order to define the exact position of the "zero time" channel it was necessary to obtain simultaneous events in the muon and electron telescopes. This was done by removing the target and disconnecting the anticoincidence channels $\bar{2}$ and $\bar{3}$; muons which passed through both telescopes produced the required coincidences.

Under the above conditions events were obtained in a single channel of the kicksorter, which was thereby defined as the "zero time" channel. It was not known, however, where "zero time" lay within the channel, so that its position had only been defined to an accuracy of $1/72$nd of the time base length. By adjustment of the back bias control of the kicksorter, it was possible to make the "zero time" events appear equally in two adjacent channels. The adjustment

was very sensitive, and "zero time" was defined by this means to an accuracy of one-thirtieth of a channel width.

Periodic checks were made during the experiment on the position of "zero time", and whenever necessary the back bias was re-adjusted to bring it back to its correct position between two channels. The adjustments required corresponded to an over-all instability in the position of "zero time" of less than 10 mμsec. This instability had no detrimental effect on the accuracy of the lifetime measurements, but had to be taken into account in the experiment described in Chapter II.

2 k) Calibration of the Timesorter

Timesorter time base ranges of 2, 3.5, 5 and 12 μsec were used to cover the various mean lives being measured. Each range was calibrated, at intervals throughout the experiment, by the use of a variable delay double pulse generator. The time delay between the two pulses was adjusted so that the kicksorter counted equally in two adjacent channels; by this means the timesorter output was known to one-thirtieth of a channel. The time delay was measured by displaying the two pulses on a Tektronix type 545 oscilloscope, the time base of which was calibrated accurately against a standard frequency waveform. It was estimated that the over-all accuracy of calibration was 0.5%: the difference between separate calibrations of the same time base range was never greater than 1% during the entire experiment.

* * *

## SECTION 3 : ELECTRONIC TECHNIQUES

### 3 a) The Coincidence Circuit and Associated Amplifiers

The complete electronic system is shown in block diagram form in Fig. 2. Photomultipliers of the type used are incapable of giving substantial pulses directly into the 130 ohm signal cables. Simple head amplifiers were used, having gains little greater than unity, but capable of feeding the 130 ohm load presented by the signal cables. The head amplifier outputs were fed by way of line amplifiers having gains of 7, to the coincidence circuit. Counters 3 and 4 each fed a pair of line amplifiers in parallel, one amplifier for the coincidence pulse and the other for the anticoincidence pulse required from each. The pulses applied to the coincidence circuit had rise times and decay times of the order of 10 mμsec and 40 mμsec respectively.

The coincidence circuit was of the distributed anode line type and was designed by Cassels et al. The author designed a circuit of similar type, but this was not readily applicable to the present experiment. A discussion of the working principles applies equally well to either circuit.

A distributed transmission line was built up from the anode capacities of the coincidence valves and small centre tapped coils. This line had an impedance of 270 ohm, and a frequency cut-off of approximately 340 Mc/sec. The coincidence valves were each run at a constant current; so that a negative pulse of sufficient height to any one valve produced a positive pulse of definite height on the anode line. For two valves switched off simultaneously a pulse of twice this height was obtained on the anode lines, etc. The bias

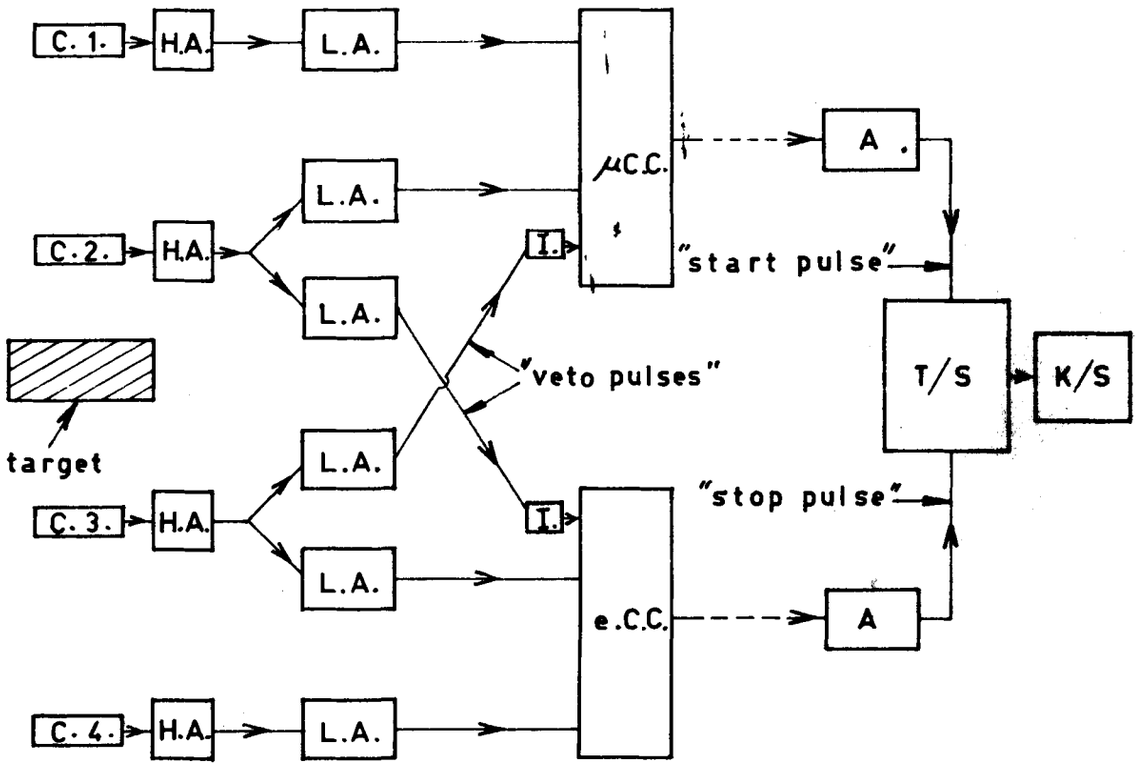


KEY

C.1. = counter 1, etc.

L.A. = line amplifier.

H.A. = head amplifier

I. = pulse inverting transformer

A = amplifier

T/S = timesorter

K/S = kicksorter

μC.C. = coincidence circuit associated with muon detection.

e.C.C. = coincidence circuit associated with electron detection.

Fig. 2 Schematic diagram of electronic system.

on the diode at the end of the anode line could be remotely adjusted to discriminate against a single, double or triple coincidence. A coincidence of the required order gave a pulse which passed through the diode, was amplified, and thence fed to the counting room. After further amplification the pulse was fed to a scalar, or the timesorter.

The anticoincidence valves were run close to cut-off. The output pulses from the line amplifiers were negative in sign, but positive pulses were applied to the anticoincidence valves by the use of inverting transformers. The anticoincidence valves thus produced negative pulses on the anode line and thereby had a "vetoing" action.

The pulses to the coincidence circuit were clipped by means of shorted cables $2\frac{1}{2}$ metres and 4 metres long connected to the grids of the coincidence and anticoincidence valves respectively. With the above clipping cable lengths the circuit had a measured resolving time of the order of 30 m$\mu$sec.

The "start" pulses and "stop" pulses had rise times of approximately 60 m$\mu$sec on arrival at the timesorter. These rise times were partly due to the attenuation of the higher frequency components of the pulses in the long signal cables between the experimental room and the counting room. Further reference will be made to the rise times in the discussion of the instability of "zero time" [Chapter II, Section 2 h)].

3 b) The Timesorter

The working principle of the timesorter is shown schematically in Fig. 4. At the heart of the circuit are two valves run in series. The lower valve is run at a constant current defined by the potential difference of 300 V across its cathode resistance.

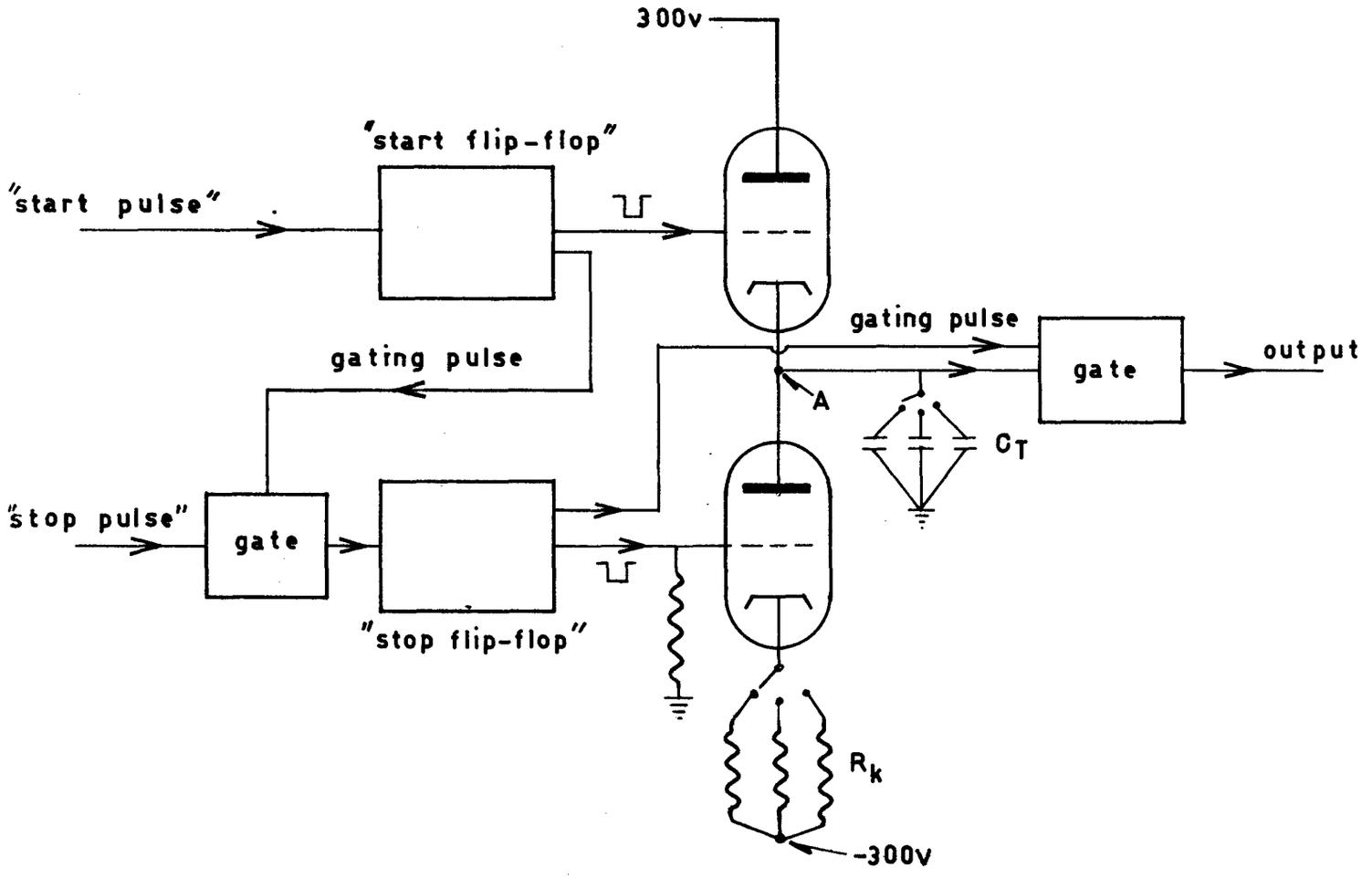


Fig. 4 Schematic diagram of timesorter.

The potential at the point A is set by the potential applied to the grid of the top valve, under the cathode follower action of the valve. The incoming "start" and "stop" pulses feed into monostable flip-flop, which have adjustable triggering levels. The input to the "stops" flip-flop is gated by the output from the "starts" flip-flop, so that a "stop" pulse can only occur if a "start" pulse is in existence at the time.

On the arrival at the timesorter of a "start" pulse of the required height the "start" flip-flop produces a square pulse, negative in sign, approximately 20 $\mu$sec long and 60 volts high, which switches off the top series valve. In this condition the time base condenser $C_t$ discharges through the lower series valve at constant current, thus giving a linear decrease with time of the potential at point A. The arrival of a "stop" pulse of the required height triggers the "stop" flip-flop, which switches off the lower series valve and thereby causes the discharge of $C_t$ to cease. The potential at A then remains constant until the pulse from the "starts" flip-flop comes to an end, when the upper series valve rapidly recharges $C_t$, bringing the potential at A back to its original value. As a result of the above process a pulse is produced at A with a height proportional to the time delay between the two input pulses.

The pulse from A is fed by way of a gate to the kicksorter, the gate being opened by pulses from the "stops" flip-flop. Thus an event can only be obtained on the kicksorter if both a "start" pulse and a "stop" pulse have been received by the timesorter. Without the above, gate events of maximum height would have been obtained on the kicksorter whenever a "start" count occurred on its own; this would have given a kicksorter counting rate far in excess of the value with which it could cope.

Various time base ranges were obtained by adjustment of the values of the condenser $C_t$, and the resistance $R_t$. Each time base used was found to be linear within the accuracy of the method of calibration, i.e. to $\frac{1}{2}\%$.

The "start" and the "stop" flip-flops each have rise-times of approximately 120 mμsec, in the region of their operation before triggering. This means that the instant of triggering depends to some extent on the height of the input pulses. The above rise-time is the main factor giving rise to instability in the position of "zero time".

3 c) Setting Up Procedure

Each counter was plateaued on singles, by observing the height of the output pulses from the coincidence circuit on a kick-sorter, for the counter placed in the full energy pion beam. On adjustment of the E.H.T. it was apparent that there was a clearly defined E.H.T. setting above which the pulses from the coincidence circuit (other than small pulses arising from photomultiplier noise) were of nearly constant height, this setting being known as the "knee" of the counters E.H.T. plateau. Counter 1 was required to detect muons; its E.H.T. was set at 150 V above the knee of its plateau. Counters 3 and 4 had to detect electrons, and counter 2 had to veto electrons which passed right through the apparatus; in the three cases the electrons would be close to minimum ionizing. Each of the three counters was run at 250 V above the knee of its E.H.T. plateau in order to allow for the difference in light output from the scintillator between electrons and pions passing through the counter.

The above method for plateauing counters is to be recommended over the conventional method in which the counting rate is measured on a scalar as a function of E.H.T., in that by the former

the knee is defined independently of discriminator settings, and a clear separation is obtained between pulses due to beam particles and those due to general background.

The counters were delayed with respect to each other by observing counting rates as a function of the delay inserted in the signal cable of one of the counters; delays were inserted by means of a remotely controlled delay box giving delays of from 0 to 20 metres of signal cables.

With the counters correctly delayed the coincidence circuit outputs were observed on the kicksorter, for pairs of counters in coincidence, and the following points were noted:

i) the pulses had a small range of heights around 20 V, and no change was observed when the E.H.T.'s of both counters were increased by several hundred volts, i.e. both counters were already well plateaued;

ii) with only one counter switched on no output was observed on the kicksorter, i.e. the coincidence circuit was correctly discriminating against "singles".

At the beginning of each day the heights of the pulses were checked on the kicksorter for single and double coincidences to make sure that none of the levels or gains had drifted in the electronic system.

* * *

## SECTION 4 : EXPERIMENTAL RESULTS

### 4 a) General

Approximately 7 hours running time was given to each target, the time was split up into 2 or 3 intervals, and the kicksorter counts were taken down at the end of each interval. This procedure guarded against the loss of an excessive amount of data in the event of a failure in the kicksorter.

The numbers of events seen by the muon telescope, the electron telescope and the kicksorter were recorded by scalers. From the first two numbers the random coincidence rate between the two telescopes could be calculated, thus checking the value given by the kicksorter channels preceding "zero time".

In order to minimize the possibility of human error, readings were made by two independent observers on each occasion on which data was taken. Counts were read off the kicksorter on "scale of 8", and the numbers were converted to "scale of 10" by the use of tables. The random background was subtracted from the counts in each channel, and two different methods of analysis were applied.

### 4 b) Graphical Analysis

Results were plotted on semi-logarithmic graph paper, counts per channel being plotted against channel number. An example of such a graph is given in Fig. 5 for the case of muons stopped in vanadium. Had there been a single exponential present, the points would have fallen on a straight line, but in practice the line is curved due to the presence of a small amount of carbon background.

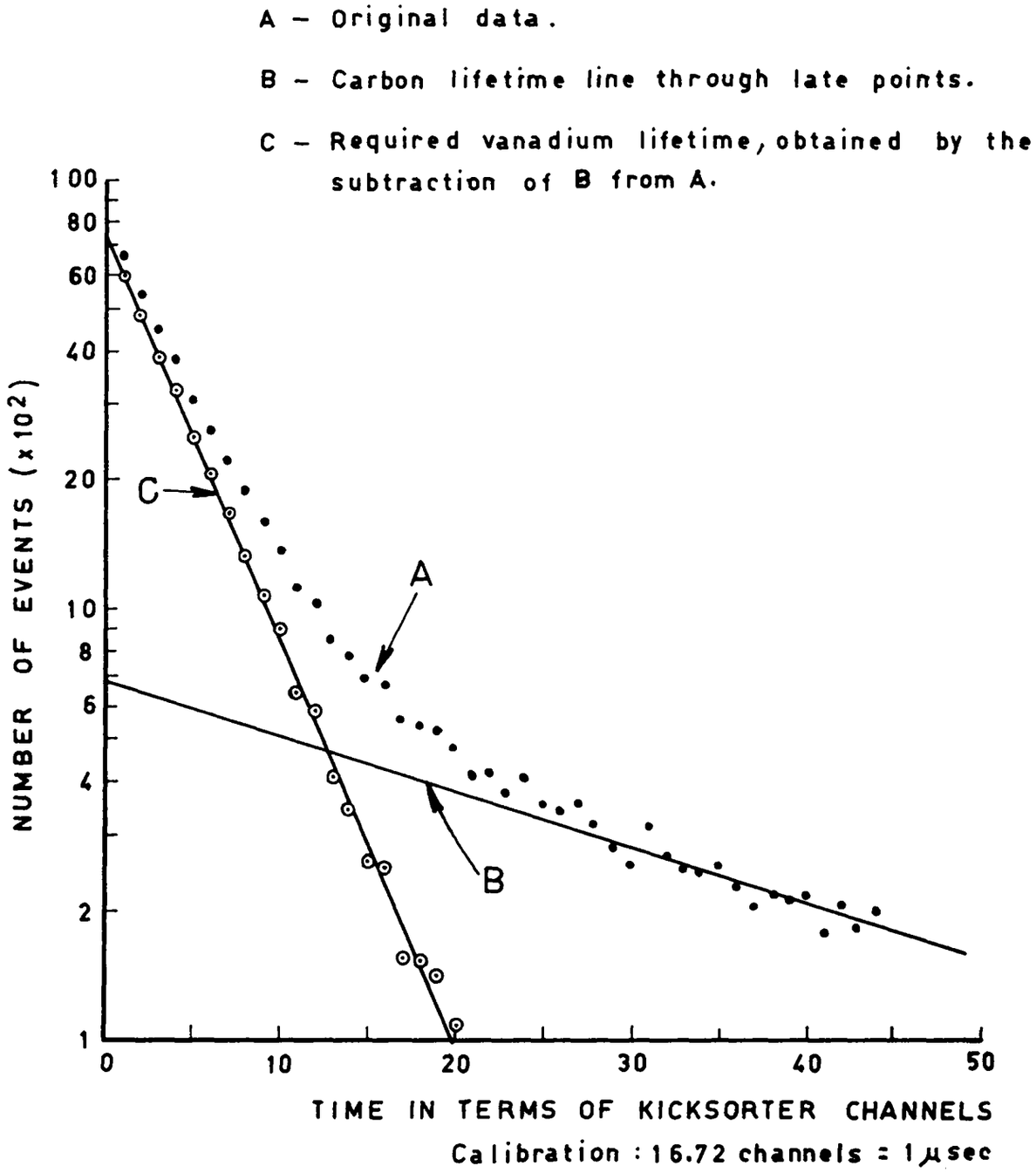


Fig.5 Histogram of kicksorter counts against time, showing graphical analysis of the result, for negative muons stopped in vanadium.

For most of the targets considered, the lifetimes being measured are very different from the muon lifetime in carbon (e.g. T(Ni) = .15 μsec and T(C) = 2.0 μsec). In such cases the late channels follow the carbon lifetime almost completely, and thus a line drawn through the late channels with the known "carbon slope" will give a fairly accurate estimate of the carbon background present. The subtraction of the carbon line from the original experimental data should give a pure exponential function having the required mean life. In practice, the points obtained by the above process were found to lie very well on a straight line as is seen in Fig. 5, in which the original data points are marked A, B is the carbon lifetime line, and the points C were obtained by the subtraction of B from A. The required muon mean life is obtained from the line C in accordance with the equation:

$$T_L = - t/\log (y_t/y_0) \qquad (20)$$

where $T_L$ is the muon mean life ($\lambda_L = 1/T_L$), $y_t$ the number of counts in channel t, and $y_0$ the number of counts in channel 0.

Kuscer, Milhailovic and Park[34] have described a graphical method for the calculation of mean lives from experimental results, in which numbers of events have been observed as a function of time. The data is grouped into 3 sums, $Y_{0\infty}$, $Y_{1\infty}$, and $Y_{2\infty}$, these being the total numbers of events beyond times $t_0$, $t_1$ and $t_2$ respectively. From the 3 sums an estimate of the mean life, almost as accurate as that given by a least squares fit, can be obtained. Optimum accuracy is attained with $t_0 \doteq 0$, $t_1 \doteq T_L$, and $t_2 \doteq 2.5T_L$.

In the case discussed by Kuscer et al. the measurements were free of background, and the fractional error in the calculated mean life was given by

$$\sigma_{T_L/T_L} = \sqrt{\frac{1.22}{N_{total}}} \qquad (21)$$

Fig.6 Experimental points and fitted curve for measurement in vanadium.

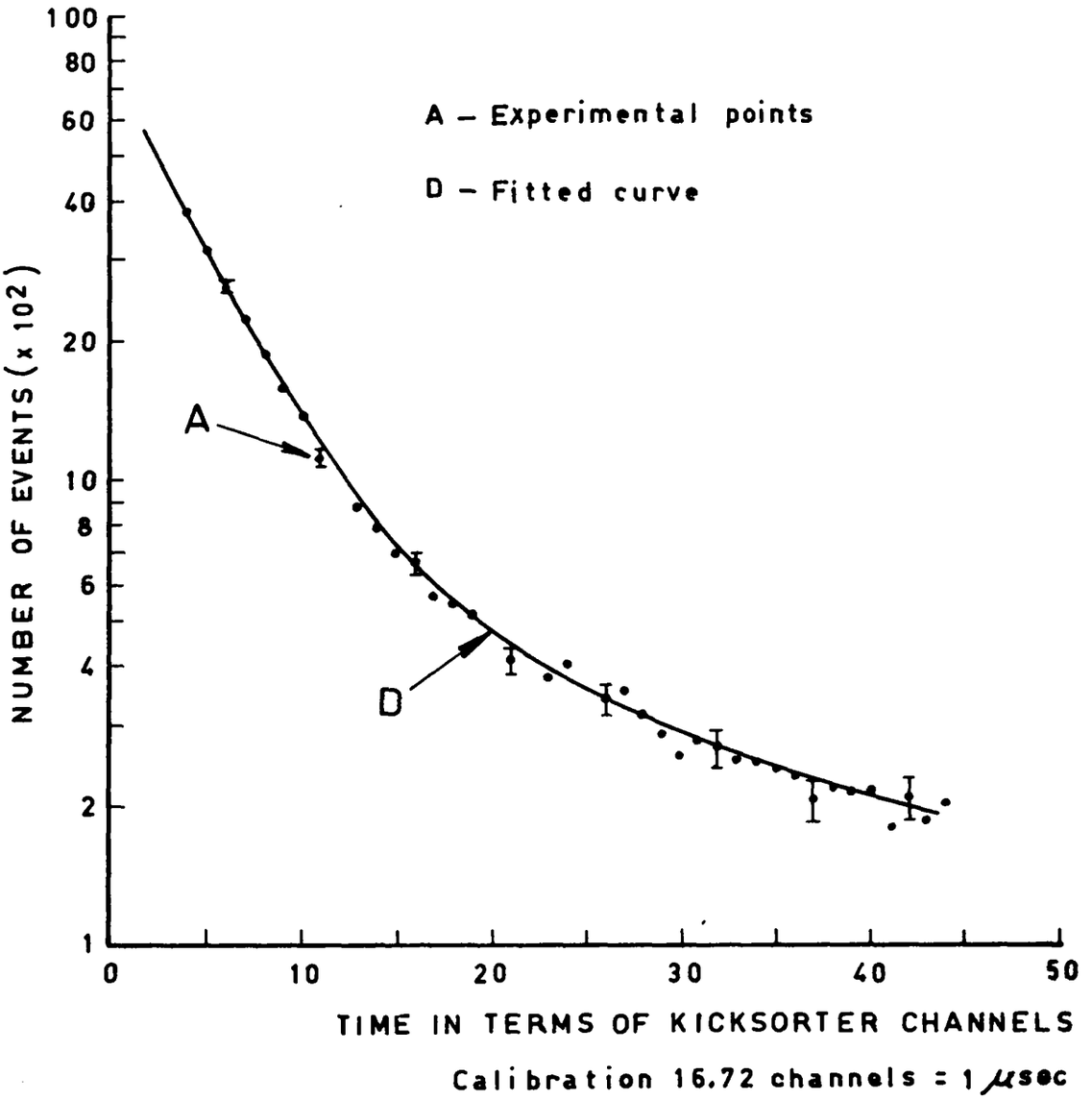

where $N_{total}$ is the total number of decay events observed and $\sigma_{T_L}$ is the standard deviation. In the present case the subtraction of the background from the experimental determined data has considerably complicated the calculation of $\sigma_{T_L}$. However, it has been possible to estimate an upper limit for the error, the calculation being discussed in Section 4 d).

4 c) Computer Analysis

A more accurate approach has been made to the problem by A. Kirk of the University of Liverpool, Department of Statistical Analysis. He has developed a programme for use with the Manchester University electronic computer, by which a best fit can be obtained to an experimental curve of the form:

$$y = A.e.^{-\lambda_1 \cdot t} + B.e.^{-\lambda_2 \cdot t}. \qquad (22)$$

The best fit was defined as that fit which gave the minimum value of $\chi^2$. The fitted curve and associated values of the constants A, B, $\lambda_1$ and $\lambda_2$ were printed out by the computer. In Fig. 6 the experimental points and the "best fit curve" are shown for the case of muons stopped in vanadium.

The muon loss rates calculated by the two different methods are in good agreement; the values given in this thesis are those calculated by means of the computer, the method being the more accurate.

4 d) Calculation of Errors

The computer method of analysing the results does not lend itself to the calculation of the statistical errors in the determined muon loss rates. Statistical errors can be calculated in the case of the "integral method" of Kuscer et al., and it is these errors which

are quoted in the results. It should be noted that the "integral method" does not make full use of the available data, and in consequence the errors calculated by it will be over-estimates of the errors actually applicable.

By use of the 3 sums $Y_{0\infty}$, $Y_{1\infty}$ and $Y_{2\infty}$ the maximum accuracy of the "integral method" can be attained. However, for the purpose of calculating errors only the first two sums will be considered. It may be shown that the error calculated by this means is only a slight over-estimate of the error applicable to the case in which all 3 sums are considered.

The muon mean life is given by:

$$T_L = t_1/\log_e(Y_{0\infty}/Y_{1\infty}). \qquad (23)$$

The standard deviation in the mean life is obtained from Eq. 23 by partial differentiation, and is given by

$$(\sigma_{T_L}/T_L)^2 = \left[(\sigma_{01}/Y_{0\infty})^2 + (Y_{01}/Y_{0\infty})^2 \times (\sigma_{1\infty}/Y_{1\infty})^2\right] \Big/ \left(\log_e \frac{Y_{0\infty}}{Y_{1\infty}}\right)^2 \qquad (24)$$

where $\sigma_{01}$ and $\sigma_{1\infty}$ are the standard deviations in the numbers $Y_{01}$ and $Y_{1\infty}$, taking into account the subtracted backgrounds and their associated errors.

The calculated values of the fractional errors in the mean lives were in all cases, apart from fluorine, of the order of 1%.

The calibrations of the timesorter were considered to be accurate to $\frac{1}{2}$%, but in order to allow for the possibility that slight changes in the timesorter time base occurred with time, it will be assumed that the calibrations of the various time bases are uncertain to 1%.

The over-all fractional errors in the measured muon loss rates are of the order of 1½%; it should be noted that these errors are the optimum usefully attainable by the existing apparatus, having regard to cyclotron running time requirements.

4 e) Tabulated Results

In Table III the results of the present experiment are shown. In column 2, muon loss rates $\lambda_L$ are given in terms of kick-sorter channels, in column 3 the relevant timesorter calibrations are noted, and in column 4 the resulting loss rates are given in terms of actual time. The total numbers of decay events observed for each target considered are noted in column 5.

TABLE III

Muon Loss Rates ($\lambda_L$).

| Element | $\lambda_L$/ time width of channels | Timesorter calibration channels/ $\mu$sec | $\lambda_L$ ($\times 10^5$/sec) | Total number of decay events observed |
|---|---|---|---|---|
| fluorine | 0.0635(±2.9%) | 11.38(±1%) | 7.22±0.22 | 30,000 |
| aluminium | 0.2186(± 1 %) | 5.23(±1%) | 11.40±0.16 | 70,000 |
| calcium | 0.1890(±0.8%) | 16.56(±1%) | 31.3 ±0.4 | 51,000 |
| vanadium | 0.2142(±1.7%) | 16.72(±1%) | 35.8±0.7 | 31,000 |
| manganese | 0.2678(±1.5%) | 16.78(±1%) | 44.9±0.8 | 25,000 |
| cobalt | .1973(±1.3%) | 27.95(±1%) | 55.1±0.9 | 24,000 |
| nickel | 0.2360(±1.5%) | 28.05(±1%) | 66.1±1.2 | 15,000 |
| copper | 0.2351(±0.7%) | 27.42(±1%) | 64.5±0.8) | 28,000 |

The required capture rates $\lambda_c$ may be obtained from the measured loss rates $\lambda_L$ by the subtraction of the relevant decay rates $\lambda_d$. The experiment of Chapter II has established that muons bound in copper, and in aluminium, decay at the same rate as free muons, within the statistical errors of the experiment. All the elements for which loss rates have been measured in the present work lie below copper in the periodic table. Although the detailed behaviour of the 'bound muon' decay rate is not known, it is reasonable to assume that it will be a monotonic function of Z. It may therefore be expected that the 'bound muon' decay rates in the elements between copper and aluminium will also be approximately equal to the free muon decay rate. The accepted value of the free muon decay rate [$\lambda_d = (4.50 \pm .05) \times 10^5/\text{sec}$] [33] has been used in the calculation of capture rates. (Account has been taken of the errors in the measured $\lambda_d(Z)$.)

In Table IV a comparison is made between the capture rates obtained in the present experiment[31], the results of Sens et al.[30] and the rates predicted by Primakoff. A better fit to our data can be obtained from Primakoff's theory by using modified values of the parameters $\gamma\lambda_c(1,1)$ and $\delta$, viz. $\gamma\lambda_c(1,1) = 141$ and $\delta = 2.85$. The figures thus obtained are given in parentheses in column 2. (For Table IV, see page 37.)

In Table V the ratios $\lambda_c(\text{element})/\lambda_c(\text{Ca})$ obtained in the present experiment are compared with the ratios calculated by Tolhoek and Luyten[3], and the values obtained in the experiment of Sens et al. The present results are again seen to be in good agreement with those of Sens et al., and both show a preference in favour of the ratios predicted for Gamow-Teller coupling.

The ratios given for pure Gamow-Teller and Fermi couplings are slightly misleading if in fact a mixture of the two interactions

TABLE IV

Muon Capture Rates

| Element | Predictions of Primakoff ($\times 10^5$/sec) | Present exp. ($\times 10^5$/sec) | Exp. of Telegdi et al. ($\times 10^5$/sec) |
|---|---|---|---|
| F | 1.68 (1.75) | 2.72 ± 0.5 | 2.54 ± 0.22 |
| Al | 6.60 (6.61) | 6.90 ± 0.3 | 7.85 ± 0.44 |
| Ca | 27.8 (28.0) | 26.8 ± 0.5 | 25.1 ± 0.9 |
| V | 29.2 (33.2) | 31.3 ± 0.7 | 33.4 ± 0.8 |
| Mn | 37.4 (39.9) | 40.4 ± 0.8 | 37.3 ± 1.2 |
| Co | 46.3 (49.8) | 50.6 ± 0.9 | |
| Ni | 58.6 (61.0) | 61.6 ± 0.2 | 58.8 ± 1.9 |
| Cu | 54.5 (58.5) | 60.0 ± 0.8 | 67.9 ± 2.2 |

TABLE V

Ratios of capture rates for certain pairs of elements

| Elements being compared | Ratios predicted by Tolhoek and Luyten | | | Present experiment | Experiment of Telegdi et al. |
|---|---|---|---|---|---|
| | S,V coupling | T,A coupling | Equal amounts of S,V and T,A coupling | | |
| V/Ca | 0.77 | 1.03 | 0.97 | 1.17±0.03 | 1.33±0.10 |
| Mn/Ca | 0.95 | 1.43 | 1.31 | 1.51±0.04 | 1.48±0.08 |
| Co/Ca | 1.14 | 1.85 | 1.67 | 1.89±0.05 | |
| Ni/Ca | 1.34 | 2.21 | 1.99 | 2.29±0.06 | 2.34±0.12 |

is present. This is due to the fact that $\lambda_c(T,A)$ is approximately three times as large as $\lambda_c(S,V)$, and so the ratio is weighted towards that for pure Gamow-Teller interaction. To illustrate this a column is included in Table V giving the ratios $\lambda_c$(element)/$\lambda_c$(Ca) (calcium) for equal amounts of Fermi and Gamow-Teller interactions (i.e. with $C_F = C_{G.T.}$).

* * *

## SECTION 5 : CONCLUSIONS

One is now confronted with the problem of whether the agreement between our present results and the predictions of Tolhoek and Luyten definitely establishes that muon capture is a Gamow-Teller interaction. It must also be remembered that the present results are in good agreement with Primakoff's calculations, which do not take into account the type of coupling present. If one considers Table I of Tolhoek and Luyten's paper, it will be seen that in the case of Fermi coupling the transition probabilities from definite initial to definite final nuclear states fluctuate rather violently in going from one transition to another. On the other hand, for Gamow-Teller coupling the variations in the transition probability are much less violent. If Fermi coupling were to occur the muon capture rate would not vary smoothly with the atomic number of the target nucleus, and Primakoff's formula would not give a satisfactory fit. One might suggest that it is fortuitous that Gamow-Teller coupling occurs in nature, resulting in a fairly smooth variation of muon capture rate with atomic number, and allowing Primakoff's simple model to give excellent predictions.

However, it is difficult to reconcile the present results with the current hypothesis of a universal Fermi interaction involving a mixture of vector and axial vector couplings. This conclusion is, of course, subject to the tentative nature of the calculations of Tolhoek and Luyten.

It is of interest to compare the absolute values of the predicted and measured capture rates, in order to determine the value of the coupling constant $g_{\mu c}$. The most reliable result is obtained by making the comparison for calcium, from which we derive:

$$g_{\mu c} = \left[ (g^{F}_{\mu c})^2 + 3(g^{GT}_{\mu c})^2 \right]^{\frac{1}{2}} = (4.3 \pm 0.4) \times 10^{-49} \text{ erg cm}^3. \qquad (25)$$

The error takes into account known uncertainties in the theory.

Beta decay and muon decay behave with a certain 'Universality'; both have V-A type coupling, and the vector coupling constants are equal for the two. This equality has been explained by Feynman and Gell-Mann in the 'conserved vector current' hypothesis[2]. The same value of the vector coupling constant is expected to apply in the case of muon capture, i.e.

$$g^{F}_{\mu c} = g^{F}_{\mu d} = g^{F}_{\beta d} = (1.41 \pm .01) \times 10^{-49} \text{ erg cm}^3. \qquad (26)$$

From Eqs. (25) and (26) we obtain the ratio between the Fermi and Gamow-Teller coupling constants in muon capture:

$$\left| g^{GT}_{\mu c} / g^{F}_{\mu c} \right| = 1.67 \pm 0.2 \qquad (27)$$

which may be compared with the ratio for $\beta$ decay:

$$g^{GT}_{\beta d} / g^{F}_{\beta d} = 1.25 \pm .04 \ . \qquad (28)$$

Hence we find the ratio between the Gamow-Teller coupling constants for muon capture and beta decay:

$$X^{GT} = \left| g^{GT}_{\mu c} / g^{GT}_{\beta d} \right| = 1.34 \pm 0.2 \ . \qquad (29)$$

$X^{GT}$ has been measured in a more direct manner in the experiment of Godfrey[35], and in the more accurate experiment of Lundby et al.[36]. The quantity they measured was the ratio between the rates of the two processes $\mu^- + C_{12} \rightarrow B_{12} + \nu$ and $B_{12} \rightarrow C_{12} + e^- + \bar{\nu}$. In

both interactions a Gamow-Teller transition between the ground states of the two nuclei predominates, and thus the nuclear parts of the matrix elements are the same. Godfrey calculated a theoretical ratio of 228 between the transition rates, assuming $g^{GT}_{\mu c} = g^{GT}_{\beta d}$. Lundby et al. obtained an experimental ratio of 312 ± 18 and hence deduced a ratio between the coupling constants:

$$X^{GT} = g^{GT}_{\mu c} \Big/ g^{GT}_{\beta d} = 1.17 \pm 0.04 \ . \qquad (30)$$

It is seen that the result of the present experiment is consistent with that of Lundby et al.

It should be noted that according to Eq. (27) Gamow-Teller coupling will contribute 8.3 times as much as Fermi coupling to the capture rate in calcium; this would explain why the experimental ratios of capture rates (see Table V) agree closely with the ratios predicted for pure G.T. coupling.

One may wonder whether the apparent difference between the G.T. coupling constants of muon capture and $\beta$ decay implies a failure of 'Universality'. However, the present calculations of muon capture rates are very tentative, and there are two effects, not considered by Tolhoek and Luyten, which may have increased the effective G.T. coupling constant. These are:

i) an induced pseudoscalar coupling[37] brought about by a muon capture process transmitted by an intermediate pion

$$\mu^- + p \rightarrow \pi^- + p + \nu \rightarrow n + \nu .$$

This gives rise to an effective pseudoscalar coupling, with a coupling constant approximately 8 times as large as the vector coupling constant for the normal capture process ($C_p \doteq 8\ C_V$).

ii) On the hypothesis of a "conserved vector current"[2] we expect direct pion-lepton interactions of the type:

$$\pi^+ + \mu^- \rightarrow \pi^0 + \nu .$$

Arising from these interactions we expect multi-stage muon capture processes.

Effects i) and ii) may each produce changes of the order of 20% in the predicted capture rates.

It may be hoped that more complete calculations will be made, allowing 'Universality' to be checked more precisely for the muon capture interaction.

* * *

# CHAPTER II

## THE PERTURBATION OF MUON DECAY BY ATOMIC BINDING

## SECTION 1 : INTRODUCTION

Negative muons brought to rest in matter are captured into atomic orbit around the target nuclei, and thence cascade rapidly down to ground state orbits. The classical K-orbit radius for a muon is a factor $m/\mu$ smaller than that for an electron (the nucleus being taken as a point charge), and is given by:

$$r_K = \hbar/\mu c\alpha Z \qquad (30)$$

where $\hbar$ is Planck's constant $/2\pi$, $\mu$ is the muon mass, $\alpha$ is the fine structure constant and Z is the atomic number of the binding nucleus. In copper, for example, $r_K$ is $8.7 \times 10^{-13}$ cm, which is approximately $\frac{3}{2}$ times the nuclear radius. The Coulomb binding energy at such a small radius is several MeV.

There are three effects which may be expected to modify the muon decay rate $\lambda_d(Z)$ in the bound state:

a) the volume in phase-space available to the decay particles will be reduced, because the energy available for the interaction is less by several MeV (the binding energy of the muon);

b) the muon decays whilst in motion in the mesic atom, and it will therefore appear to live longer in the lab. system as a result of time dilation;

c) the wave-function of the emitted electron will be perturbed by the Coulomb field of the nucleus. This will cause a change in the energy spectrum of the electron and in the over-all decay rate $\lambda_d(Z)$.

Effects a) and b) each cause a decrease in the decay rate. Effect c), which is similar to the Coulomb effect in $\beta$ decay, increases the decay rate. However, the Coulomb effect will be smaller in magnitude in the case of $\mu$ decay due to the fact that the electron has a much higher energy and starts life on average further from the centre of the nucleus than in $\beta$ decay. The order of magnitude of effects a) and b) may be estimated as follows.

a) The volume in phase-space available to muon decay varies approximately as the fifth power of the available energy (W), the final system having five degrees of freedom. Classically, and for a point nucleus, the energy of a particle of charge e orbiting around a nucleus of charge Ze is given by

$$\text{B.E.} = -Ze^2/2r \tag{31}$$

where r is the radius of the orbit (assumed circular). In the case of the ground state of a $\mu$-mesonic atom, the binding energy becomes $-\mu Z^2\alpha^2c^2/2$. The energy available to the decay particles is the sum of the rest energy of the muon $\mu c^2$ and the binding energy. The ratio between bound and free muon decay rates due to effect a) is thus given by

$$\lambda_d^{a)}(Z)\Big/\lambda_d(0) = W^5/W_0^5 = [\mu c^2(1-Z^2\alpha^2/2)]^5/(\mu c^2)^5 . \tag{32}$$

To the first order in $Z^2\alpha^2$ we have:

$$\lambda_d^{a)}(Z) = \lambda_d(0)(1 - \tfrac{5}{2} Z^2\alpha^2) . \tag{33}$$

b) Assuming a circular orbit, the muon has a kinetic energy equal in magnitude to its binding energy and a velocity $\beta=v/c$ given by the equation

$$\sqrt{1-\beta^2} = (\text{rest energy/total energy}) = \mu c^2/\mu c^2(1+Z^2\alpha^2/2). \tag{34}$$

As a result of its motion the muon will appear to live longer in the laboratory system. The observed decay rate $\lambda_d^{b)}(Z)$ is related to the intrinsic decay rate in the rest system of the muon by the relation:

$$\lambda_d^{b)}(Z) = \lambda_d(0)\sqrt{1-\beta^2} = \lambda_d(0)(1+Z^2\alpha^2/2)^{-1} \qquad (35)$$

i.e. to the first order in $Z^2\alpha^2$

$$\lambda_d^{b)}(Z) = \lambda_d(0)(1-Z^2\alpha^2/2) \ . \qquad (36)$$

Combining effects a) and b) we have:

$$\lambda_d^{a)b)}(Z) = \lambda_d(0)(1-\eta Z^2\alpha^2), \text{ with } \eta = 3. \qquad (37)$$

The calculation given above is a considerable over-simplification of the problem. A complete analysis would use the exact phase-space relation for the muon decay process, and would have to include an integration over all possible momentum states of the initial muon. It would also have to take into account the finite size of the nucleus.

A calculation of effects a) and b) has been made by Khuri and Wightman for the case of a point nucleus[38]. They obtained a result similar to Eq. (37) above, but with $\eta = 5.16$. No details of their calculation are available. Huby and Newns have also calculated effects a) and b) for the case of an extended nucleus, but using only a mean value for the muon momentum[39]. Their result is similar to Eq. (37) but with Z replaced by $Z_{effective}$ (Tiomno and Wheeler, 1949)[32], and with $\eta = 4.4$.

There are no calculations available on effect c), the perturbation of the decay electron's wave-function by the Coulomb field.

Fierz and Yamaguchi[40] have suggested that the decay rate may be expected to show a dependence of the type:

$$\lambda_d^{c)}(Z) = \lambda_d(0)[1 + k(E_{Coulomb}/E_{kinetic})] \qquad (38)$$

where $E_{Coulomb}$ is the perturbing energy arising from the Coulomb field at the point of creation of the electron, $E_{kinetic}$ is the energy of the unperturbed electron, and k is a positive constant of the order unity. According to this equation an increase in the decay rate of the order of 10% may be expected in the case of a copper target, as a result of effect c). It is interesting to note that according to the formula of Huby and Newns, effects a) and b) produce a decrease in the decay rate of 12% for a copper target. It would therefore appear that effect c) may tend to cancel effects a) and b) for muons stopped in copper or elements of similar Z.

In view of the uncertain state of the theory it was decided to measure $\lambda_d(Z)$ experimentally, as this quantity is required in the deduction of muon capture rates from the measured muon loss rates of Chapter I. Three elements were chosen for the measurements, namely: copper, aluminium and carbon. The copper was selected as it was the element of highest Z considered in the experiment of Chapter I, and it seemed reasonable to suggest that if the muon decay rate was unchanged in copper, then it would be unaffected in all the other elements of lower Z. Carbon was chosen for the purpose of comparison, as the change in the decay rate produced by each of the three effects a), b) and c) could be negligible for so low a Z. The aluminium was chosen in order to ascertain whether any unexpected effects occurred at an intermediate value of Z.

The method by which $\lambda_d(Z)$ was measured is discussed in the next section.

* * *

## SECTION 2 : EXPERIMENTAL METHOD

### 2 a) Principle of the Measurement

The quantity to be measured was the perturbed decay rate of negative muons brought to rest in a target (Z). It was not possible to measure $\lambda_d(Z)$ directly because of the existence of the competing capture process, which contributes to a net muon loss rate:

$$\lambda_L(Z) = \lambda_c(Z) + \lambda_d(Z) \ . \qquad (39)$$

It was however possible to measure $\lambda_d(Z)$ indirectly by observing the fraction $F_d(Z)$ of stopped muons which gave rise to decay electrons:

$$F_d(Z) = \lambda_d(Z)/[\lambda_c(Z) + \lambda_d(Z)] = \lambda_d(Z)/\lambda_L(Z) \ . \qquad (40)$$

The required decay rate $\lambda_d(Z)$ is the product of a muon loss rate (measured in the experiment of Chapter I) and the quantity $F_d(Z)$. In principle $F_d(Z)$ could be measured by bringing a known number of muons to rest in a target and observing the number of decay electrons emitted. In practice, it is difficult to obtain i) a cyclotron beam with a muon content known to sufficient accuracy, or ii) an electron telescope having a sufficiently well-defined detection efficiency, to make such an experiment worth while.

In both the methods finally adopted ratios of decay rates $[R(Z_1/Z_2) = \lambda_d(Z_1)/\lambda_d(Z_2)]$ were measured, for pairs of elements of rather different atomic number. In this way neither the absolute muon content of the beam nor the absolute detection efficiency of the electron telescope were required to be known.

2 b) "Alternate Target Method"

For the purpose of the present thesis the following definitions will be made:

i) target thicknesses will be measured in gm per $cm^2$

$$t_{gm/cm^2} = t_{cm} \times \rho \ ,$$

where $\rho$ is the density of the target material;

ii) the stopping ability of a material for particles of energy E is defined as the energy loss of the particles in passing through 1 $gm/cm^2$ of the material

$$\text{Stopping ability } S(E) = (dE/d\xi)_E \ ;$$

iii) the stopping power of a target, for particles of a specified type, is defined as the energy the particles must have to just pass through the target.

In the "alternate target method" two targets of approximately equal stopping power, and of similar geometry, were used. Muon decays were observed for each target with $\mu^+$ and $\mu^-$ beams incident, using the apparatus described in Chapter I, Section 2. The various runs were monitored by use of the muon telescope. A total of four runs were made, viz:

1) $\mu^-$ on carbon - $N_C^-$ decay events observed;
2) $\mu^+$ on carbon - $N_C^+$ decay events observed;
3) $\mu^-$ on copper - $N_{Cu}^-$ decay events observed;
4) $\mu^+$ on copper - $N_{Cu}^+$ decay events observed;

where the numbers $N_C^-$, $N_C^+$, $N_{Cu}^-$ and $N_{Cu}^+$ are all normalized to the same number of muon telescope counts. In the cases of runs 2) and 4) all the muons which stopped in the target will have decayed (positive

muons do not get close enough to the target nuclei to undergo capture). Thus the numbers $N_C^+$ and $N_{Cu}^+$ will be equal unless:

a) different numbers of muons stopped in the two targets, in spite of the fact that the same numbers of monitor counts were considered in the two cases; or

b) the over-all detection efficiency of the electron telescope was different in the two runs (due mainly to geometrical differences between the two targets).

Let $\delta_C^-$, $\delta_{Cu}^-$ and $\delta_{Cu}^+$ be the fractions of the $12\bar{3}$ counts which correspond to muons stopping in the target in the cases of runs 1,2,3 and 4 respectively, and let $\epsilon_C^-$, $\epsilon_C^+$, $\epsilon_{Cu}^-$, $\epsilon_{Cu}^+$ be the relevant electron detection efficiencies for the four runs. From the above definitions we have:

$$\frac{N_{Cu}^+}{N_C^+} = \frac{\delta_{Cu}^+}{\delta_C^+} \times \frac{\epsilon_{Cu}^+}{\epsilon_C^+} \tag{41}$$

and

$$\frac{N_{Cu}^-}{N_C^-} = \frac{\delta_{Cu}^-}{\delta_C^-} \times \frac{\epsilon_{Cu}^-}{\epsilon_C^-} \times \frac{F_d(Cu)}{F_d(C)} \, . \tag{42}$$

From Eqs. (41) and (42) we have by multiplication:

$$\frac{F_d(Cu)}{F_d(C)} = \frac{N_{Cu}^-}{N_C^-} \times \frac{N_C^+}{N_{Cu}^+} \left( \frac{\delta_{Cu}^-}{\delta_C^-} \times \frac{\delta_C^+}{\delta_{Cu}^+} \right) \left( \frac{\epsilon_{Cu}^-}{\epsilon_C^-} \times \frac{\epsilon_C^+}{\epsilon_{Cu}^+} \right) . \tag{43}$$

If the $\mu^+$ and $\mu^-$ beams have identical momentum spectra and if each beam has a time invarient muon content, then both the bracketed terms will equal unity, and Eq. (43) will reduce to:

$$\frac{F_d(Cu)}{F_d(C)} = \frac{N_{Cu}^-}{N_C^-} \times \frac{N_C^+}{N_{Cu}^+} \, . \tag{44}$$

The ratio between the muon decay rates in the two target materials will be given by:

$$\frac{\lambda_d(Cu)}{\lambda_d(C)} = \frac{N^-_{Cu}}{N^-_C} \times \frac{N^+_C}{N^+_{Cu}} \times \frac{\lambda_L(Cu)}{\lambda_L(C)} . \qquad (45)$$

Although the above experiment was made and a result obtained, it was later decided that the two assumptions with regard to the beam characteristics were unjustified, and would require to be tested experimentally. In view of the greater simplicity and reliability of the "sandwich target method" it was then decided to abandon the above "alternate target method".

2 c) "Sandwich Target Method"

Laminated targets were made up from alternate sheets of two materials. The targets considered were copper with aluminium, copper with carbon, and aluminium with carbon. For a given target (e.g. Cu-Al) decay events were observed, using the experimental arrangement previously discussed, for negative muons brought to rest in the target. A pattern was obtained on the kicksorter representing a curve of the form

$$N_t = N_0(Cu)e^{-\lambda_L^{Cu}\cdot t} + N_0(Al)e^{-\lambda_L^{Al}\cdot t} + R.B.G. \qquad (46)$$

where $\lambda_L^{Cu}$ and $\lambda_L^{Al}$ are the muon loss rates in copper and aluminium respectively, $N_t$ is the number of decay events occurring in the $t_{th}$ kicksorter channel, and $N_0(Cu)$ and $N_0(Al)$ are the numbers of decay events occurring in the "zero time channel" as a result of muons which stopped in copper and aluminium respectively.

It should be noted that there is no spurious carbon lifetime present, this background having been eliminated by the use of large targets (see Chapter I, Section 4 h).

We have, in effect, a mixture of two exponentials, one being characteristic to negative muons stopped in copper, and the other to negative muons stopped in aluminium. The two exponentials have very different mean lives [$T_L(Cu) = .15$ $\mu$sec and $T_L(Al) = .8$ $\mu$sec] and it is therefore fairly simple to separate them.

By means of the above experiment the two numbers $N_o(Cu)$ and $N_o(Al)$ were obtained. The relative number of muons which stopped in the Cu and Al may be calculated from a knowledge of the plate thickness and the stopping abilities of the two materials. Let this calculated ratio be $r(Cu/Al)$. Then the ratio between the total number of decay events observed in copper and the total number observed in aluminium is given by:

$$\frac{N_o(Cu)T_L(Cu)}{N_o(Al)T_L(Al)} = \frac{F_d(Cu)}{F_d(Al)} \times r(Cu/Al) \qquad (47)$$

(because $N_{total} = N_o T_L$).

Substituting from Eq. (40) we obtain:

$$\frac{\lambda_d(Cu)}{\lambda_d(Al)} = \frac{1}{r(Cu/Al)} \frac{N_o(Cu)}{N_o(Al)} \times \frac{\lambda_L(Cu)T_L(Cu)}{\lambda_L(Al)T_L(Al)} \qquad (48)$$

$$\text{i.e. } \frac{\lambda_d(Cu)}{\lambda_d(Al)} = \frac{1}{r(Cu/Al)} \frac{N_o(Cu)}{N_o(Al)} \qquad (\because \lambda_L \times T_L = 1). \qquad (49)$$

Hence the required ratio of decay rates is obtained from the measured ratio $N_o(Cu)/N_o(Al)$, and the calculated ratio $r(Cu/Al)$.

The advantage of the sandwich target method is that it is self-normalizing, the information on the decay in both elements being built up over the same period of time, with the same beam and electron telescope conditions applying to the two elements.

2 d) Target Details

The various targets were made up of 9" × 9" sheets of material, the physical details of which are given below. It should be noted that the plate thicknesses were calculated from the measured masses and areas of the plates.

| i) Cu-Al target | 30 Cu plates | 30 Al plates |
|---|---|---|
| Total mass of plates | 3956.5 gm | 1844.2 gm |
| Plate thickness | .252 gm/cm$^2$ | .117 gm/cm$^2$ |
| Total thickness of material | 7.56 gm/cm$^2$ | 3.53 gm/cm$^2$ |
| Purity | 99.8% | 99% |
| Calculated ratio of muons stopped | 1.73 : 1 | |

| ii) Cu-$CH_2$ target | 32 Cu plates | 32 $CH_2$ sheets |
|---|---|---|
| Total mass of plates | 4220.8 gm | 1076.8 gm |
| Plate thickness | .252 gm/cm$^2$ | .0643 gm/cm$^2$ |
| Total thickness of material | 8.05 gm/cm$^2$ | 2.06 gm/cm$^2$ |
| Purity | 99.8% | 99.5% |
| Calculated ratio of muons stopped | 2.16 : 1 | |

| iii) Al-$CH_2$ target | 27 Al plates | 27 $CH_2$ sheets |
|---|---|---|
| Total mass of plates | 3318.0 gm | 1228.3 gm |
| Plate thickness | .235 gm/cm$^2$ | .087 gm/cm$^2$ |
| Total thickness of material | 6.35 gm/cm$^2$ | 2.35 gm/cm$^2$ |
| Purity | 99% | 99.5% |
| Calculated ratio of muons stopped | 1.84 : 1 | |

The criterion which was applied in deciding upon the plate thicknesses to be used was that muons should come to rest in a fair number of plates of both materials, in order to minimize "quantization

effects", i.e. if muons stopped in, say, four plates only, then there would be every possibility that one material would be favoured over the other from the point of view of the total number of muons stopped and the mean electron detection geometry.

Although the energy spectrum of the negative muon beam has not been accurately determined, measurements by ourselves and by Cassels et al. have indicated that all the muons can be stopped within a 10 gm/cm$^2$ thick paraffin target. The sandwich targets were therefore designed to have stopping powers approximately equal to that of 10 gm/cm$^2$ of paraffin. The use of some 60 sheets of the two materials in each target will have adequately guarded against the above-mentioned "quantization effects".

A lower limit was put on the plate thicknesses that could be used by the requirement that the range-energy and energy loss relations be accurately known down to these thicknesses.

For each target the ratio of thicknesses of the two materials was adjusted so as to give approximately twice as many muons stopping in the material of higher Z (the material giving the larger muon loss rate); this facilitated the separation of the two exponentials from the experimental data.

Polythene sheets were used for the experiments in which carbon was required to be present, as it would have been difficult to obtain pure carbon sheets of the required thickness and uniformity. The resulting presence of hydrogen will have had a negligible effect on the measured ratio $\frac{\lambda_d(Z)}{\lambda_d(C)}$ .

2 e) Calculation of the Relative Numbers of Muons Stopped in the Two Materials of the Sandwich Targets[1]

For the purpose of the calculation it was assumed that the energy spectrum of the muons leaving the bending magnet (i.e. entering counter 1) was square. This assumption does not, in fact, effect the generality of the calculation. The problem then reduced to that of finding a set of muon energies ($E_0'$, $E_1'$, $E_2'$, etc.) corresponding to muons which came to rest at the various intersurfaces of the target (see Fig. 7). Muons having energies in the ranges $E_0'$ to $E_1'$, $E_2'$ to $E_3'$, etc., will have stopped in copper, and those with energies $E_1'$ to $E_2'$, $E_3'$ to $E_4'$, etc., will have stopped in aluminium. The ratio between the total number of muons stopped in copper and the total number stopped in aluminium is given by:

$$r(Cu/Al) = (B'_{01} + B'_{23} + B'_{45} + \dots)/(B'_{12} + B'_{34} + B'_{56} + \dots) \quad (50)$$

where $B'_{01} = E'_1 - E'_0$, etc.

The required energy differences $B'_{ab}$ were obtained by first calculating the corresponding energy differences $B_{ab} = E_b - E_a$ for muons leaving counter 2, and then taking into account the effect of the intervening paraffin absorber.

The $B_{ab}$ were calculated on the basis of the model shown in Fig. 8, in which successive copper and aluminium plates were considered to be added to the front surface of the target, and for each plate added an energy difference $B_{ab}$ and a new total energy $A_b$ were calculated using energy loss data. According to this model the stopping plate was always the same material (viz. copper) and the front plate of the target alternated between aluminium and copper, whereas in the physical situation the front plate was always copper, and the stopping plate alternated between the two materials. Small corrections were applied to the derived energy differences to take account of this difference.

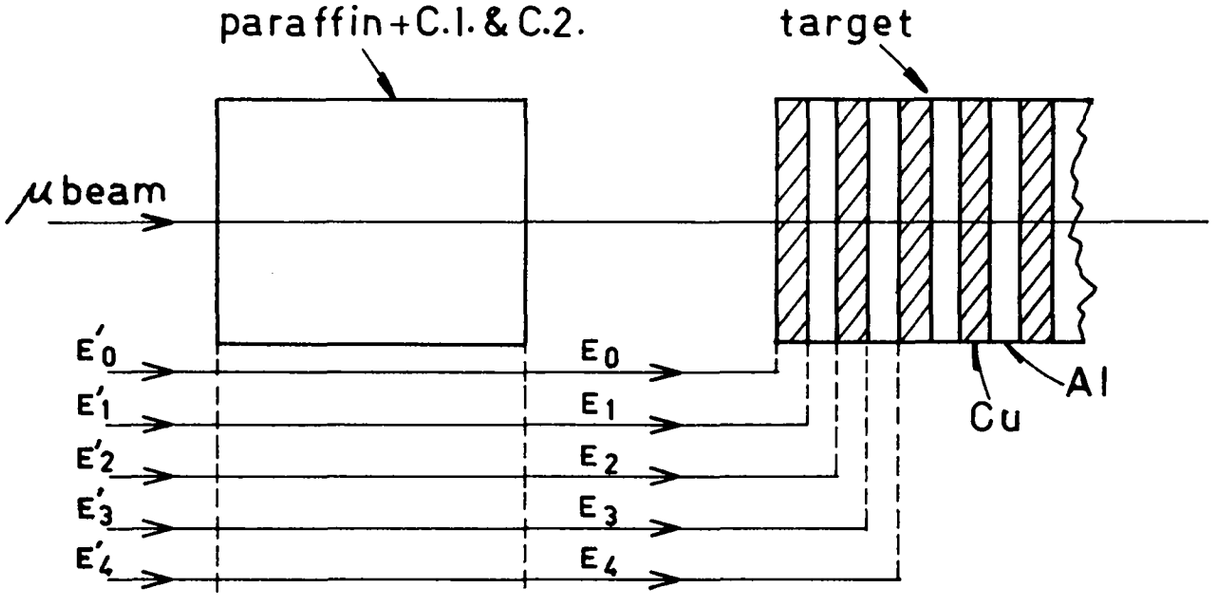


Fig.7 Energies required for muons to reach the various intersurfaces of the Cu–Al sandwich target.

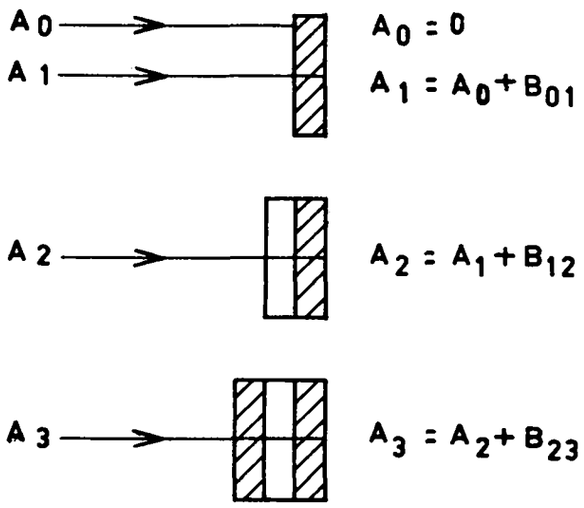


Fig.8 Energy matrix.

The results of the calculations are given below:

Cu-Al target : $r(Cu/Al) = 1.73 \pm .02$

$Cu-CH_2$ target : $r(Cu/CH_2) = 2.16 \pm .04$

$Al-CH_2$ target : $r(Al/CH_2) = 1.84 \pm .04$

The errors quoted arise from uncertainties in the energy loss data used[41].

2 f) Gamma-ray Detection Efficiency of the Electron Telescope

The evaluation of the ratio $\lambda_d(Z_1)/\lambda_d(Z_2)$ depends on the measurement of the relative number of decay electrons emitted from the two materials of the sandwich target. However, if the electron telescope were sensitive to neutrons and $\gamma$-rays, then we would no longer be looking at the required muon decays alone, but also at capture events in which the excited daughter nuclei emitted neutrons or $\gamma$-rays.

Approximately 92% of muons brought to rest in copper are captured, the remaining 8% undergoing decay (i.e. there are 13 times as many captures as decays). The multiplicity of neutrons emitted per muon capture in copper is of the order of 2, and the $\gamma$ multiplicity is of the order of 3, and thus approximately 25 times as many neutrons, and 40 times as many $\gamma$-rays, as electrons will have reached the electron telescope. There was 1 gm of copper between counters 3 and 4 which was sufficient to prevent neutrons from being detected by the knock-on of a proton from one counter to the other.

It was calculated that $\gamma$-rays above 2.5 MeV could produce Compton electrons having sufficient range to pass from one counter to the other, and for $\gamma$-rays above 3 MeV the detection efficiency was shown to be of the order of 1%. This result was confirmed

experimentally by the use of radio-active $\gamma$-ray sources, and also using the University of Liverpool H.T. set. It was not possible to proceed with a detailed calculation of the probability of detecting a $\gamma$-ray, per muon capture, because the shape of the $\gamma$-spectrum was not known. From the figures given above one might estimate that approximately 25% of the events observed in copper were in fact due to $\gamma$-rays.

In aluminium the capture rate is approximately equal to the decay rate, and so the effect due to the $\gamma$-rays will be only 2% or 3%. In carbon the capture rate is much smaller than the decay rate and so the effect of the $\gamma$-rays will be negligible.

### 2 g) Measurement of the Relative Number of Gamma-rays Detected by the Electron Telescope

An extra counter was added to the experimental arrangement, being placed between the target and the electron telescope. The new counter (counter 5) was run in anticoincidence with counters 1 and 2, in order to veto beam particles which passed right through the target.

'Decay events' were observed for muons stopped in a pure copper target, runs being made with, and without, counter 5 in anti-coincidence with the electron telescope. The 'decay events' observed in the first run must have been due to $\gamma$-rays only, as electrons emitted from the target would have been vetoed. The number of events observed with counter 5 on was a factor $3.13 \pm 0.1$ smaller than the number observed with counter 5 off. This means that only $68.2\% \pm 1\%$ of the events previously observed from copper were in fact true muon decay events.

This result was confirmed by a similar measurement on the Cu-$CH_2$ sandwich target.

From these results corrections were calculated to the measured ratios $N_0(Z_1)/N_0(Z_2)$ :

1) Cu-Al target : multiply $N_0(Cu)/N_0(Al)$ by .717 ± .01
2) Cu-$CH_2$ target : multiply $N_0(Cu)/N_0(CH_2)$ by .682 ± .01
3) Al-$CH_2$ target : multiply $N_0(Al)/N_0(CH_2)$ by .952 ± .002

2 h) Instability of "Zero Time"

The numbers $N_0(Z_1)$ and $N_0(Z_2)$ were obtained from the experimental data by extrapolation back to "zero time". It was possible to determine the position of "zero time" to a great accuracy by means of the method described in Chapter I, Section 4 e). It was found, however, that the position was not completely stable, and drifts of the order of one-tenth of a kicksorter channel were noted over periods as short as twenty minutes.

The instability was due to the rather long rise-times (120 mμsec) of the "start" and "stop" flip-flops. The triggering levels of the two flip-flops were set to one-third of the height of the incoming pulses, and under these conditions a change of 10% in pulse height would cause a change of 4 mμsec in the instant of triggering of a flip-flop, to which corresponds a change of one-tenth of a channel in the position of "zero time". It was suggested that the drift in "zero time" simply corresponded to fluctuations in the gains of the coincidence circuits and their associated amplifiers.

It was decided to treat "zero time" as a statistical quantity having a normal distribution of errors, and to observe its behaviour experimentally. Its position was measured every two hours, throughout the experiment, and from the results the mean position of "zero time" ($\bar{Z}$) and the standard deviation of the mean ($\sigma_{\bar{Z}}$) were calculated. These two quantities are listed below for the three targets considered:

| Target | Z (K/S channels) | $\sigma_{\bar{Z}}$ |
|---|---|---|
| Cu-Al | 13.506 | .036 |
| Cu-$CH_2$ | 13.49 | .034 |
| Al-$CH_2$ | 14.51 | .022 |

The uncertainty in the position of "zero time" gave rise to the following fractional errors in the determined ratios $R(Z_1/Z_2)$ :

| Target | $\sigma_R/R(Z_1/Z_2)$ |
|---|---|
| Cu-Al | 1.2% |
| Cu-$CH_2$ | 1.2% |
| Al-$CH_2$ | 0.3% |

where $R(Z_1/Z_2) = \lambda_d(Z_1)/\lambda_d(Z_2)$.

2 i) Constant Background Discrepancies

Several measurements were made with the timesorter on an extended time base range, in order to check the method of measuring the random background in the channels preceding "zero time". The time base range was chosen to be of such a length that all the exponential quantities would have died away over the first half of the range, leaving the second half for the measurement of random background only. It was found in each case investigated that the constant background given by the late channels exceeded that given by the channels preceding "zero time" by approximately 20%.

Further measurements were made with the apparatus looking at random coincidences only (i.e. with the muon and electron telescopes placed in different parts of the experimental room) and the counts in the early and late channels were found to be in good agreement.

No explanation has been arrived at for the discrepancies noted above; they may be due to a defect in the electronic system or to the presence of a mysterious exponential quantity with a mean life of the order of 20 $\mu$sec.

Wilmot et al. have used a kicksorter of the same design in their measurements of $\gamma$-ray spectra. They have noticed some discrepancies in the events obtained in the early channels and have therefore made it their practice to ignore the information in the first dozen channels of the kicksorter which were, in fact, the very channels used by us for the measurement of the random background.

Our experiments were therefore designed to place as little reliance as possible on the random background measured in the channels preceding "zero time". In the case of the muon loss rate measurements of Chapter I, the time base ranges were required to be of sufficient length to allow a measurement of the background to be made in the late channels of the kicksorter.

In the sandwich target experiments it was not possible to use time bases of sufficient length for the longer mean life to have died away by the late channels, as this would have entailed having the exponential with the shorter mean life extending over too few channels. It was decided to treat the results as if the constant background were completely unknown.

A computer programme was developed by A. Kirk, by which a best fir could be found to the experimental points assuming a theoretical curve of the form:

$$N_t = N_0(Z_1)e^{-\lambda_L(Z_1)t} + N_0(Z_2)e^{-\lambda_L(Z_2)t} + C \qquad (51)$$

where C is the unknown constant background.

The best fit was defined as that giving the minimum value of $\chi^2$. Known values of $\lambda_L(Z_1)$ and $\lambda_L(Z_2)$ were inserted into the programme, in order to obtain the best possible accuracy for $N_0(Z_1)$ and $N_0(Z_2)$. It was apparent that if a reliable value of C had been available, then the over-all accuracy of the experiment would have been considerably improved. The values of $\lambda_L(Z)$ used were, in the cases of copper and aluminium, those obtained by the experiment of Chapter I. In the case of polythene the value obtained by Sens et al. for carbon ($\lambda_L = 4.96 \pm .05 \times 10^5/\text{sec}$) was used[30].

In the case of the Al-$CH_2$ measurement the problem of separating the two exponentials proved very difficult due to the similarity of the two lifetimes and the uncertainty in the constant background. The accuracy of the final result was too poor to publish; it may be noted, however, that it was not in conflict with the expected value of unity, within the large experimental errors.

## 2 j) Effect of Parity Violation

As a result of the non-conservation of parity in the muon decay interaction the decay electrons are emitted anisotropically. The angular distribution of the electrons is given by:

$$W(\Theta) = k(1 - |P| \alpha \cos \Theta) \qquad (52)$$

where $\Theta$ is the angle between the muon beam direction and the direction of emission of electrons, $|P|$ is the magnitude of polarization of the muon beam at the instant of decay, and $\alpha$ is the asymmetry parameter having a theoretical value of .33 for the case in which the complete spectrum of decay electrons is considered.

Measurements on negative muons stopped in matter indicate that they become completely depolarized if the target nuclei have non-zero spins. If the nuclei have zero spins then the residual

polarization of the muons, on reaching the K atomic orbits, is of the order of 20% [42].

Of the three materials used in the experiment, only the carbon has a nuclear spin of zero (the presence of the hydrogen in the polythene will have had a negligible effect). Thus parity violation will have effected only those parts of the data involving muons stopped in the $CH_2$. The asymmetry coefficient $|P|\alpha$ has a measured value of .040 ± .005 for $\mu^-$ in carbon [42].

In the presence of a magnetic field muons precess with a frequency $f = \vec{H}\cdot\vec{\mu}$, where $\vec{\mu}$ is the muon magnetic moment in Bohr Magnetons. Such a precession will have caused a periodic fluctuation to be superimposed on the $CH_2$ decay exponential, resulting in a composite decay curve of the form:

$$N_t(CH_2) = N_0(CH_2)[1 - .04Q \cos(2\pi f \cdot t)]\, e^{-\lambda_L(CH_2)\cdot t} \qquad (53)$$

where Q is a geometrical factor taking into account the angular acceptance of the electron telescope, and having a calculated value of .74 ± .10 for the present apparatus.

There was a magnetic field of 14 Gauss in the region of the target, to which corresponds a precession period of the muon of approximately 6 μsec. In the case of the Cu-$CH_2$ measurement a time base of 3 μsec was used, so that a stopped muon will have precessed through 180° during the sweep of the time base. The effect of parity violation will thus have been to lower $N_0(CH_2)$ by 3% and to raise $N_{3\mu sec}(CH_2)$ by 3%, which to a first approximation will have made $\lambda_L(CH_2)$ appear smaller by 4%. A modified value of $\lambda_L(CH_2)$ was therefore used in the computer programme. Finally it was necessary to multiply the computed value of $N_0(CH_2)$ by the correction factor $\delta_p = 1.03 \pm .01$.

* * *

## SECTION 3 : RESULTS

### 3 a) Cu-$CH_2$ Target

In Fig. 9 a histogram is shown of the numbers of counts recorded in the various kicksorter channels, for the measurement with the Cu-$CH_2$ target. The points represent the experimentally determined numbers, and the continuous line represents the fitted curve:

$$N = N_0(Cu)e^{-\lambda_L(Cu)\cdot t} + N_0(CH_2)e^{-\lambda_L(CH_2)\cdot t} + C \qquad (54)$$

the constants $\lambda_L(Cu)$ and $\lambda_L(CH_2)$ having been given the respective values of $64.5 \pm 0.8 \times 10^5$/sec and $4.78 \pm .07 \times 10^5$/sec. The curve fitting was made under the requirement that $\chi^2$ be a minimum; the curve obtained had a value of $\chi^2$ lying within the normally imposed acceptance limit of "5% probability". The values derived for the remaining constants were as follows:

$$\frac{N_0(Cu)}{N_0(CH_2)} = 3.332 \ (\pm 4.5\%)$$

$$C = 416$$ (compare with the value C = 354 obtained from early kicksorter channels).

The quoted error in the ratio $N_0(Cu)/N_0(CH_2)$ takes into account

i) the statistical errors in the experimental points;
ii) the uncertainty in the position of "zero time"; and
iii) the standard deviations of the muon loss rates used.

The three effects give fractional errors of 3.8%, 1.2% and 2.2% respectively in the measured ratio, yielding a total error of 4.5%.

Fig.9 Histogram of kicksorter counts against time, showing the experimental points and fitted curve for the measurement on $Cu-CH_2$

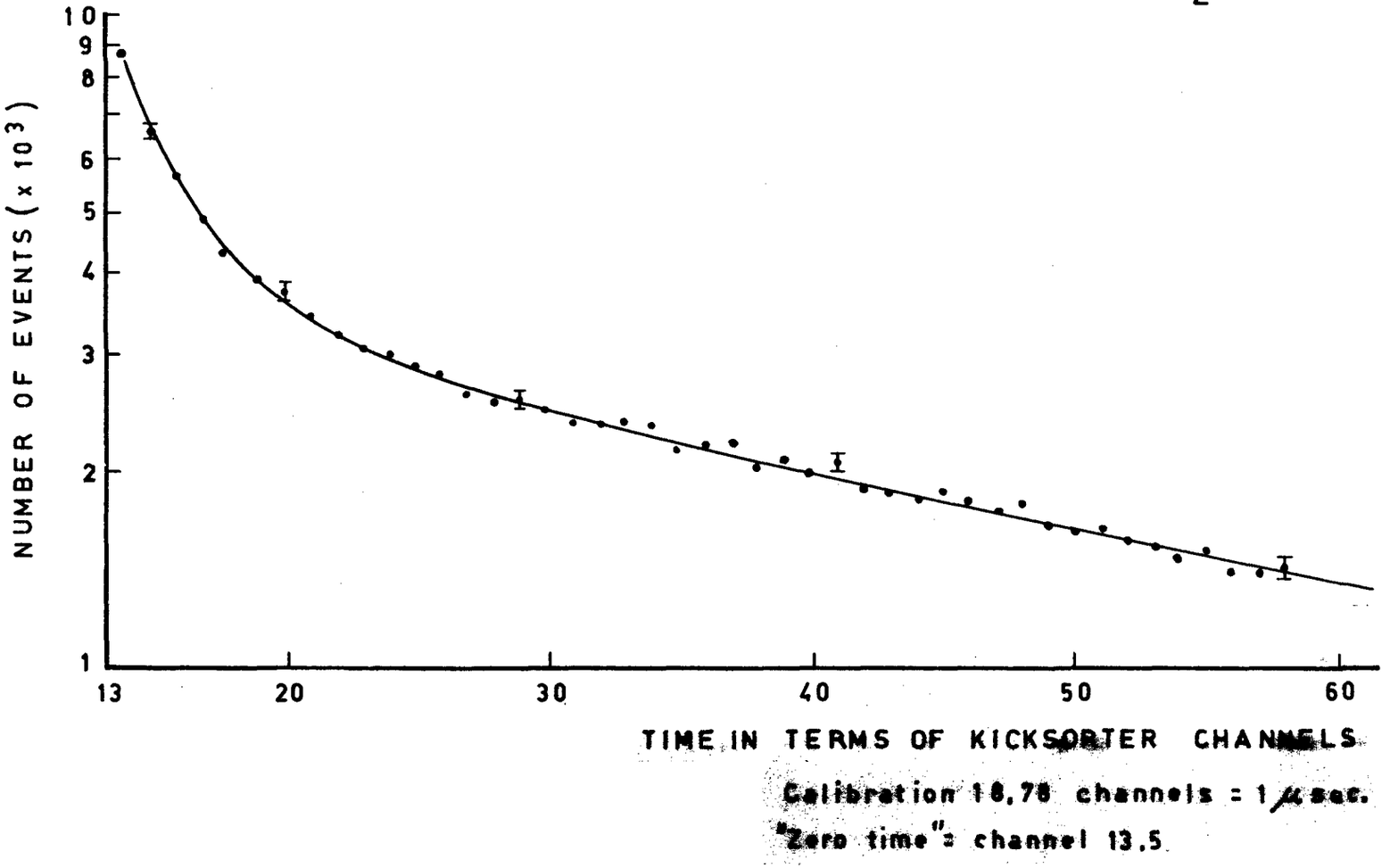

The required ratio of decay rates $R(Cu/CH_2)$ is given by the equation:

$$R(Cu/CH_2) = \frac{N_o(Cu)}{N_o(CH_2)} \times \frac{\gamma}{\delta_p} \times \frac{1}{r(Cu/CH_2)} \qquad (55)$$

where $\gamma$ is the correction factor taking into account the $\gamma$-ray detection efficiency of the electron telescope, and $\delta_p$ corrects for the reduction in $N_o(CH_2)$ brought about by parity violation.

The factors in the above expression have the following values:

$$\gamma = .682 \ (\pm 1.5\%)$$
$$\delta_p = 1.03 \ (\pm 1\%)$$
$$r(Cu/CH_2) = 2.16 \ (\pm 2\%) \ .$$

Hence the required ratio may be calculated:

$$R(Cu/CH_2) = 1.02 \pm .05 \ . \qquad (56)$$

3 b) Cu-Al Target

The result has been treated in a similar manner to that for $Cu\text{-}CH_2$. The curve fitting was made with the values of $\lambda_L(Cu)$ and $\lambda_L(Al)$ specified as $64.5 \pm .8 \times 10^5$/sec and $11.40 \pm .16 \times 10^5$/sec respectively. The fitted curve had a value of $\chi^2$ lying within the "5% probability" acceptance limit. The following values were derived for the constants:

$$\frac{N_o(Cu)}{N_o(Al)} = 2.44 \ (\pm 5.5\%)$$

$C = 311$ (compare with the value $C = 283$ obtained from early kicksorter channels).

The remaining factors required for the calculation of R(Cu/Al) have the following values:

$$\gamma = 0.717 \ (\pm 1.5\%)$$
$$\delta_p = 1$$
$$r(Cu/Al) = 1.727 \ (\pm 1\%) \ .$$

Hence we calculate:

$$R(Cu/Al) = 1.016 \pm 0.06 \ . \qquad (57)$$

* * *

## SECTION 4 : DISCUSSION AND CONCLUSION

The relative magnitudes of the two opposing effects [a) + b), and c)] disturbing the muon decay process are not well known. However, both effects increase with increasing Z, and so both should be very small in the case of carbon. Thus the measured ratio $R(Cu/CH_2)$ gives essentially the ratio between the decay rate in copper and that in free space:

$$\text{i.e. } \lambda_d(Cu) = (1.02 \pm 0.5)\lambda_d(0). \tag{58}$$

One may similarly argue that the effects in aluminium are expected to be small compared with those in copper, and thus the measured ratio R(Cu/Al) gives to a good approximation:

$$\lambda_d(Cu) = (1.02 \pm .06)\lambda_d(0). \tag{59}$$

The two independently measured values of the decay rate in copper are seen to be in excellent agreement.

The two measured ratios $R(Cu/CH_2)$ and R(Cu/Al) may alternatively be combined to give the decay rate in aluminium:

$$\lambda_d(Al) = (1.00 \pm .08)\lambda_d(0). \tag{60}$$

Bound muon decay rates have also been measured by Telegdi et al. in Chicago[43], and their results together with the results of the present experiment[44] are shown graphically in Fig. 10. It is seen that the two experiments are in good agreement, but it is difficult to reconcile Telegdi's result for iron with any of the other points. The iron point has been ignored in the drawing of the experimental curve. It appears that the decay rates in elements

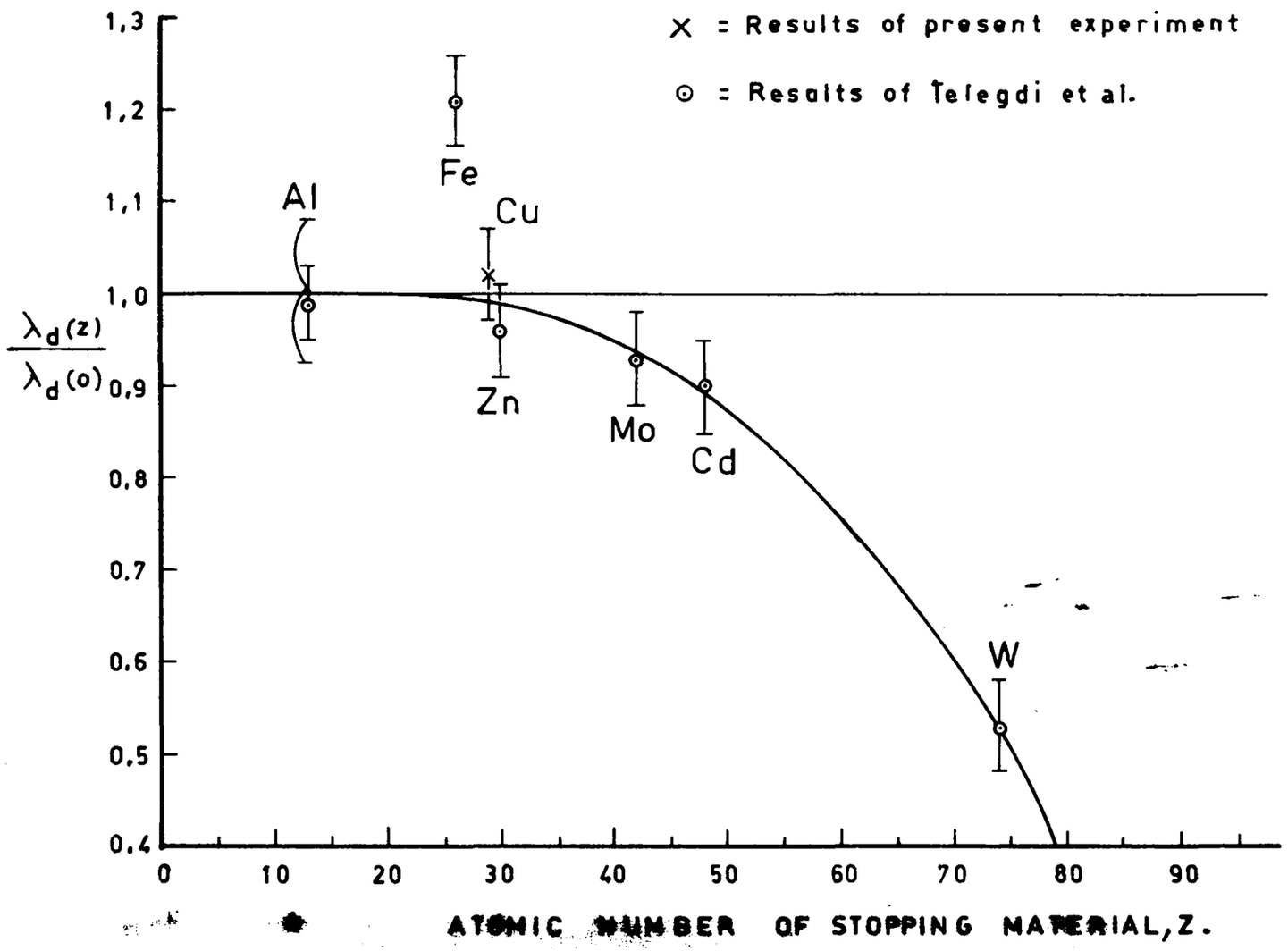


Fig. 10 Experimental curve of $\lambda_d(z)/\lambda_d(o)$ against Z.

having Z less than 30 do not differ appreciably from the free decay rate. This may be due to a cancellation between effect c), and effects a) + b). For higher Z effects a) + b) would seem to predominate, perhaps due to a saturation in effect c).

The conclusion drawn from the present experiment is that muon capture rates $\lambda_c(Z)$ may be obtained from the measured loss rates of Chapter I, $\lambda_L(Z)$, by the subtraction of the free muon decay rate.

* * *

## REFERENCES


1) G. Puppi, Nuovo Cimento 6, 194 (1949).
See also O. Klein, Nature 161, 897 (1948).

2) R.P. Feynman and M. Gell-Mann, Phys.Rev. 109, 193 (1958);
M. Gell-Mann, Phys.Rev. 111, 362 (1958).

3) H.A. Tolhoek and J.R. Luyten, Nuclear Physics 3, 679 (1957).

4) M. Goldhaber, CERN Conference on High Energy Physics (1958) p.233.

5) E. Fermi, Z.Physik 88, 161 (1934);
E.J. Konopinski and L.M. Langer, Ann.Rev.Nucl.Sci. 2, 261 (1953).

6) See, for example, F. Mandl, Quantum Mechanics, p. 203.

7) R.A. Swanson, R.A. Lundy, V.L. Telegdi and D.D. Yovanovitch, Phys.Rev.Letters 2, 430 (1959).

8) E.C.G. Sudershan and R.E. Marshak, Phys.Rev. 109, 1860 (1958).

9) See, for example, p. 227 of the article by L. Michel, Rev.Mod. Phys. 29, 223 (1957).

10) M. Fierz, Z.Physik 104, 553 (1937).

11) T.D. Lee and C.N. Yang, Phys.Rev. 104, 254 (1956).

12) C.S. Wu, E. Ambler, R.W. Hayward, D.D. Hoppes and R.P. Hudson, Phys.Rev. 105, 1413 (1957).

13) R.L. Garwin, L.M. Lederman and M. Weinrich, Phys.Rev. 105, 1415 (1957).

14) M. Goldhaber, L. Grodzins and A.W. Sunyar, Phys.Rev. 109, 1015 (1958).

15) This work has been summarized in Ref. 4), and in the lectures of C.S. Wu, Proc.Rehovoth Conf. on Nucl.Structure (1957) p.346 and of H. Frauenfelder, Varenna School on Weak Interactions (1959). The latter will be published in Nuovo Cimento.

16) W.B. Herrmannsfeldt, R.L. Burman, P. Stahelin, J.S. Allen and T.H. Braid, Phys.Rev.Letters 1, 61 (1958).

17) See the summary by O. Kofoed-Hansen, Varenna School on Weak Interactions (1959). (To be published in Nuovo Cimento.)

18) C. van der Leun, Thesis, University of Utrecht (1958).

19) A.N. Sosnovskij, P.E. Spivac, Y.A. Prokofiev, I.E. Kutikov and Y.P. Dobrynin. (To be published.)

20) M.T. Burgy, V.E. Krohn, T.B. Novey, G.R. Ringo and V.L. Telegdi, Phys.Rev.Letters 1, 324 (1958).

21) M.T. Burgy, V.E. Krohn, T.B. Novey, G.R. Ringo and V.L. Telegdi, Phys.Rev. 110, 1214 (1958).

22) L. Michel, Nature 163, 959 (1949).

23) The most recent value of $\rho = .80 \pm .02$ has been given by J. Steinberger at the Varenna School on Weak Interactions (1959). (To be published.)

24) G. Culligan, S.G.F. Frank, J.R. Holt, J.C. Kluyver and T. Massam, Nature 180, 751 (1958);
G. Culligan, S.G.F. Frank and J.R. Holt, Proc.Phys.Soc. 73, 169 (1959).

25) Experimental results include Ref. 13), and the more recent and accurate results of Steinberger et al. (Ref. 23).

26) For the theory of muon decay under parity violation, see the lecture notes of T.D. Lee, Nevis Report 50, 33 (1957); also
L. Landau, Nuclear Physics 3, 127 (1957).
A. Salam, Nuovo Cimento 5, 299 (1957).

27) T.D. Lee and C.N. Yang, Brookhaven Report 443 (T-91), p. 57 (1957).

28) A.E. Ignatenko, L.B. Egorov, B. Khalupa and D. Chultem, Joint Institute for Nuclear Research, Dubna, Report 191 (1958).

29) Measurement made by A. Astbury, M.A.R. Kemp, N.H. Lipman, H. Muirhead and R.G.P. Voss. (To be published.)

30) J.C. Sens, R.A. Swanson, V.L. Telegdi and D.D. Yovanovitch, Phys.Rev. 107, 1464 (1957).

31) A. Astbury, M.A.R. Kemp, N.H. Lipman, H. Muirhead, R.G.P. Voss, C. Zangger and A. Kirk, Proc.Phys.Soc. 72, 494 (1958).

32) The quantity $Z_{eff}^4$ has been defined in the calculations of J. Tiomno and J.A. Wheeler, Rev.Mod.Phys. 21, 153 (1949).

33) E.R. Cohen, K.M. Crowe, J.W.M. Dumond, Fundamental Constants of Physics, p. 61 (1957).

34) I. Kuscer, M.V. Mihailovic and E.C. Park, Phil.Mag. 2, 998 (1957).

35) T.N. Godfrey, Phys.Rev. 92, 512 (1953); Thesis, Princeton (1954). (Unpublished)

36) J.O. Burgman, J. Fischer, B. Leontic, A. Lundby, R. Meunier, J.P. Stroot and J.D. Teja, Phys.Rev.Letters 1, 469 (1958).

37) L. Wolfenstein, Nuovo Cimento 8, 882 (1958);
M.L. Goldberger and S.B. Treiman, Phys.Rev. 111, 355 (1958).

38) N.D. Khuri and A.J. Wightman, quoted by J.C. Sens, R.A. Lundy, R.A. Swanson, V.L. Telegdi and D.D. Yovanovitch, Bull.Am. Phys.Soc. Ser.II 3, 198 (1958).

39) Private communication.

40) Private communication.

41) M. Rich and R. Madey, UCRL Report 2301 (1954).

42) A.E. Ignatenko, L.B. Egorov, B. Khalupa and D. Chultem, Joint Institute for Nuclear Research, Dubna, Report 190 (1958).

43) R.A. Lundy, J.C. Sens, R.A. Swanson, V.L. Telegdi and D.D. Yovanovitch, Phys.Rev.Letters 1, 102 (1958).

44) A. Astbury, M. Hussain, M.A.R. Kemp, N.H. Lipman, H. Muirhead, R.G.P. Voss and A. Kirk, Proc.Phys.Soc. 73, 314 (1959).

## ACKNOWLEDGEMENTS

I am grateful to Dr. A.W. Merrison who, as my supervisor during my first year of research, introduced me to the world of high energy nuclear physics.

I must thank Prof. H.W.B. Skinner for the constant interest he has shown in my researches.

I would also like to thank Dr. B. Collinge for his work in the design of the timesorter, and for his willing advice on electronic problems; and I wish to thank Mr. K. Aitcheson for his ready and cheerful response when called upon at unusual hours to repair the pulse height analyser.

Special thanks are due to Dr. A. Kirk who devoted considerable time and energy to the development and running of a computer programme for the analysis of our results.

I must thank Mr. K. Rawlinson who ably assisted in the mechanical construction of the apparatus, and Mr. B. Halliday and the cyclotron crew for their friendly co-operation throughout the experiment.

Lastly, I must thank Messrs. T. Edge and W. Smithers of the United Kingdom Atomic Energy Authority, and Mr. W. Stevens of the Mond Nickel Company for the loan of target materials.

I am indebted to the Department of Scientific and Industrial Research from whom I received a maintenance allowance during my three years of research.

* * *